

RADIATION RESISTANCE IN RENAL CELL CARCINOMA

CARBONIC ANHYDRASE 9 AND RADIATION RESISTANCE IN
RENAL CELL CARCINOMA

By DANIEL GALLINO, B.Sc.

A Thesis Submitted to the School of Graduate Studies in Partial Fulfillment
of the Requirements for the Degree Master of Science

McMaster University © Copyright by Daniel Gallino, February 2013

McMaster University MASTER OF SCIENCE (2013) Hamilton, Ontario (Radiation Biology)

TITLE: Carbonic Anhydrase 9 and Radiation Resistance in Renal Cell Carcinoma

AUTHOR: Daniel Gallino, B.Sc. (University of Western Ontario)

SUPERVISORS: Dr. Tomas J. Farrell, Dr. Jehonathan H. Pinthus

NUMBER OF PAGES: v, 82

Abstract

Renal cell carcinoma (RCC) is the most frequently lethal of urological cancers. It arises in the lining of the proximal convoluted tubule of the kidney and is most common in men ages 50–70. Often, partial or radical nephrectomy is needed to effectively treat the disease, leaving patients with reduced kidney function. RCC frequently displays significant radiation resistance, limiting the usefulness of traditional radiation therapy which might spare patients' normal tissue. The enzyme carbonic anhydrase 9 (CA9), a product of the hypoxia pathway, is found upregulated in the majority of RCC, particularly the clear cell type. It catalyses the dissolution of carbon dioxide into water as bicarbonate and has been linked to increased invasion and migration in RCC tumour cells. The radiation resistance of two RCC cell lines 786-O (human CCRCC) and RAG (murine renal adenocarcinoma) was investigated by the clonogenic assay in the presence of a CA9 inhibitor or silencing RNA. The interference with CA9 by either of these methods significantly sensitizes 786-O cells to the effects of ionizing radiation *in vitro*. Moreover, fractionation of the dose delivered can increase this sensitization effect. It is hoped that current targeting of CA9 can make radiation therapy a more feasible option in the treatment of RCC.

Acknowledgments

I would like to express my deepest gratitude to my graduate committee...

Dr. Jehonathan Pinthus, my co-supervisor, and former employer who saw my potential and encouraged me to embark on this journey of graduate studies. These past two years, we have shared the thrill of discovery, many laughs and even a few Jewish holidays. All the while his unrelenting, can-do attitude has inspired and motivated me to exceed my own expectations.

Dr. Tom Farrell, my co-supervisor and department insider who agreed to take me on and pulled the strings to make it happen. He has helped me integrate into the department and McMaster/Juravinski Cancer Center communities and his occasional Hawaiian shirt has reminded me that research is not always serious business.

Dr. Helga Duivenvoorden who has been a much valued mentor and colleague. Never hesitating to help me develop my lab expertise and repertoire of practical assays, she has been my go-to person for any question ranging from application of scientific method to career choice. She dedicated a great deal of her own time to reviewing and improving this thesis, and I am grateful for her help.

To my colleagues...

Jian Ping Lu, who taught me all the basics of working in a biology lab. It was insightful and just plain fun to spend so much time with a person as delightfully eccentric as myself. Above all I will miss our joint singing career and plans to record a CD.

Sarah Hopmans, who courageously faced and slew untold hordes of bureaucracy required for animal testing approval. I am greatly indebted also for her help with the experimental design and execution of the animal irradiation experiments. I was not once

phased by the lack of quality audio speakers in the lab, for her ability to get songs stuck in my head is unparalleled.

Richard Hung, whose late shifts became even later while he volunteered to run the LINAC for my *in vitro* experiments. The survival curves presented here would not have been possible without his extraordinary patience. I will miss our discussions of current videogame trends that took place between hurling lethal doses of X-rays at unsuspecting cancer cells. If you listen closely, you can hear them scream.

Diana Glennie, who stayed late and ran the LINAC for my *in vivo* irradiation experiments. She has helped immensely with the organization and statistics of my thesis and scolded me relentlessly for not using “superior programs” such as LaTeX and Mendeley. I am also grateful for her providing much needed personal and moral support when this project took unexpected turns.

And to everyone else...

To my other lab mates: we've shared many good time together.

To my family and friends: your love and support has kept me motivated and grounded.

To Steam: for providing quality PC games at discounted prices when I needed them most.

And finally to the Flying Spaghetti Monster: with whom all things are possible.
Ramen.

Table of Contents

TABLE OF CONTENTS	1
LIST OF FIGURES	2
LIST OF TABLES	2
ABBREVIATIONS AND SHORTENED TERMS	3
1.0 INTRODUCTION	6
1.1 BACKGROUND.....	6
1.1.1 Renal Cell Carcinoma	6
1.1.2 RCC treatment and radiation sensitivity.....	8
1.1.3 Cell death by radiation and modes of resistance.....	10
1.1.4 Radiation resistance and hypoxia.....	13
1.1.5 RCC and hypoxia.....	14
1.1.6 Expression of carbonic anhydrase 9 as promoter of radiation resistance in RCC.....	15
1.1.7 Carbonic anhydrases	16
1.1.8 Carbonic anhydrase 9: structure.....	17
1.1.9 Carbonic anhydrase 9: expression and regulation.....	19
1.1.10 Carbonic anhydrase 9: other known functions in tumours	20
1.2 APPROACH	24
1.2.1 Targeting carbonic anhydrase 9.....	24
1.2.2 Measuring radiation resistance of RCC	26
1.2.3 Cell lines considered.....	26
1.2.4 Xenografts.....	28
1.2.5 Nude mice	29
1.3 HYPOTHESIS AND OBJECTIVES	30
1.3.1 Objectives	30
1.3.2 Hypothesis	30
2.0 METHODS	31
2.1 CELL CULTURE.....	31
2.2 MYCOPLASMA DETECTION BY DAPI (4',6-DIAMIDINO-2-PHENYLINDOLE).....	32
2.3 TRANSFECTION OF 786-O CELLS	32
2.4 PREPARATION OF PROTEIN LYSATES	34
2.5 DETERMINATION OF PROTEIN CONCENTRATION	34
2.6 WESTERN BLOT ANALYSIS	35
2.7 SURVIVAL ASSAYS	36
2.8 <i>IN VITRO</i> IRRADIATIONS	37
2.9 ACTIVITY ASSAY	37
2.10 <i>IN VIVO</i> RESISTANCE ASSAY	38
2.10.1 Animal care and monitoring	38
2.10.2 Tumour xenografts.....	38
2.10.3 Animal irradiation	39
2.10.4 Data collection	39
2.11 STATISTICS	40
3.0 RESULTS AND DISCUSSION	41
3.1 CA9 IS PRESENT IN 786-O, RAG AND LNCAP CELLS, UNDETECTABLE IN HEK CELLS	41
3.2 KNOCKDOWN OF CA9 EXPRESSION BY shRNA IN 786-O CELLS.....	42
3.3 AEBS AND shRNA CAN INHIBIT CA9 ACTIVITY <i>IN VITRO</i>	43
3.4 AEBS IS NOT TOXIC TO 786-O CELLS <i>IN VITRO</i>	46
3.5 786-O AND RAG CELLS ARE RESISTANT TO RADIATION <i>IN VITRO</i>	47
3.6 AEBS LOWERS RADIATION TOLERANCE IN 786-O AND RAG CELLS, BUT NOT IN LNCAP CELLS.....	49
3.7 786-O CELLS EXPRESSING shCA9 HAVE DECREASED RADIATION TOLERANCE	53
3.8 REDUCED CA9 EXPRESSION SENSITIZES 786-O CELLS TO RADIATION MORE SO THAN INHIBITION BY AEBS	54
3.9 AEBS OR shCA9 RADIATION TOLERANCE LOSS IS MORE PRONOUNCED IF THE RADIATION DOSE IS FRACTIONATED	55

3.10 SHCA9-EXPRESSING 786-O TUMOURS HAVE DECREASED TOLERANCE FOR RADIATION <i>IN VIVO</i>	58
4.0 CONCLUSION	64
4.1 SUMMARY.....	64
4.2 FUTURE WORK.....	66
REFERENCES	70
APPENDICES	76
APPENDIX A: SDS-PAGE AND WESTERN BLOT COMPONENTS.....	76
APPENDIX B: <i>MYCOPLASMA</i> DAPI ASSAY.....	77
APPENDIX C: SHRNA SEQUENCES.....	79

List of Figures

FIG. 1. ANATOMY OF A NORMAL KIDNEY.....	6
FIG. 2. A 3D MODEL OF A CARBONIC ANHYDRASE 9 DIMER IN A PHOSPHOLIPID BILAYER.....	18
FIG. 3. SUMMARY OF UPSTREAM EFFECTS ON, AND DOWNSTREAM EFFECTS OF CA9.....	23
FIG. 4. WESTERN BLOT ANALYSIS (SDS-PAGE RUN UNDER REDUCING CONDITIONS) FOR CARBONIC ANHYDRASE 9 IN LNCAP, 786-O, RAG AND HEK PROTEIN LYSATES.....	42
FIG. 5. WESTERN BLOT ANALYSIS (SDS-PAGE RUN UNDER REDUCING CONDITIONS) FOR CARBONIC ANHYDRASE 9 IN EIGHT 786-O SUBCLONES TRANSFECTED WITH SHCA9.....	43
FIG. 6. ACIDIFICATION OF MEDIUM OF 786-O CELLS A) IN THE PRESENCE OR ABSENCE OF AEBS B) EXPRESSING SHCA9 OR SHSCR AS DETERMINED BY THE DECREASE IN ABSORBANCE OF PHENOL RED OVER TIME.....	45
FIG. 7. TOXICITY OF AEBS TO 786-O CELLS, RAG CELLS AND LNCAP CELLS AS DETERMINED BY CLONOGENIC SURVIVAL.....	47
FIG. 8. RADIATION RESISTANCE OF 786-O CELLS, RAG CELLS, LNCAP CELLS AND LN-18 CELLS AS DETERMINED BY CLONOGENIC SURVIVAL.....	49
FIG. 9. RADIATION SENSITIVITY OF A) 786-O CELLS, B) RAG CELLS AND C) LNCAP CELLS AS DETERMINED BY CLONOGENIC SURVIVAL.....	52
FIG. 10. RADIATION SENSITIVITY OF TRANSFECTED 786-O CELLS.....	53
FIG. 11. COMPARISON OF RADIATION SENSITIZATION OF 786-O CELLS BY AEBS OR SHCA9 AS DETERMINED BY CLONOGENIC SURVIVAL.....	55
FIG. 12. RADIATION SENSITIVITY OF 786-O CELLS RECEIVING A FRACTIONATED RADIATION REGIMEN A) IN THE PRESENCE OR ABSENCE OF AEBS AND B) EXPRESSING SHRNA AGAINST CA9 AS DETERMINED BY CLONOGENIC SURVIVAL COMPARED WITH SINGLE-DOSE EXPERIMENTS.....	57
FIG. 13. AVERAGE TUMOUR SIZE BY A) VOLUME IN MM ³ AND B) WEIGHT IN GRAMS OF SUBCUTANEOUS 786-O TUMOURS.....	60
FIG. 14. WESTERN BLOT ANALYSIS (SDS-PAGE RUN UNDER REDUCING CONDITIONS) FOR CARBONIC ANHYDRASE 9 IN TUMOUR HOMOGENATES.....	61
FIG. 15. MEAN CA9 PROTEIN CONTENT IN TUMOUR XENOGRAFT HOMOGENATES.....	61
FIG. 16. REPRESENTATIVE HEMOTOXYLIN AND EOSIN STAIN OF XENOGRAFT TUMOUR TISSUE REMOVED FROM MICE.....	63
FIG. 17A. FLUORESCENCE MICROSCOPY IMAGE OF DAPI-STAINED 786-O CELLS (400X MAGNIFICATION).....	77
FIG. 17B. FLUORESCENCE MICROSCOPY IMAGE OF DAPI STAINED 786-O CELLS (BRIGHTNESS ENHANCED, 400X MAGNIFICATION).....	78

List of Tables

TABLE 1. SDS-PAGE GEL COMPONENTS AND CONCENTRATIONS.....	76
TABLE 2. SDS-PAGE BUFFERS COMPONENTS AND CONCENTRATIONS.....	76
TABLE 3. ANTIBODIES USED.....	76
TABLE 4. TRANSFECTED SHRNA SEQUENCES AND TARGETS.....	79

Abbreviations and Shortened Terms

AEBS: 4-(2-aminoethyl)benzene sulfonamide

AKT: a kinase originally discovered in the Thymoma-prone AK mouse strain

ATCC: American Type Culture Collection

ATM: Ataxia Telangiectasia Mutated protein

AUP: Animal Utilization Protocol

BALB/c: Bagg Albino mouse strain

CA: Carbonic Anhydrase

CA9/CAIX: Carbonic Anhydrase Nine

CARP: Carbonic Anhydrase-Related Protein

CCRCC: Clear Cell Renal Cell Carcinoma

CT: Computerized Tomography

cys: cystine

dH₂O: deionized Water

DMSO: Dimethyl Sulfoxide

DNA: Deoxyribonucleic Acid

dsRNA: double-stranded Ribonucleic Acid

DTT: Dithiothreitol

EGF: Epidermal Growth Factor

EGFR: Epidermal Growth Factor Receptor

FOXN1: Forkhead Box Protein

IC₅₀: Inhibitor Concentration for 50% effect

GFP: Green Fluorescent Protein

Gy: Gray (SI-derived unit of absorbed dose in Joules/Kilogram)

HIF: Hypoxia Inducible Factor

HRE: Hypoxia Responsive Element

IC: Intracytosolic

Ki: Inhibitor Constant

LET: Linear Energy Transfer

LINAC: Linear Accelerator

miRNA: micro Ribonucleic Acid

MMP: Matrix Metalloproteinase

MHC: Major Histocompatibility Complex

MRI: Magnetic Resonance Imaging

PG: Proteoglycan-like domain

PHD: Prolyl-4-Hydroxylase

PI3K: Phosphatidylinositol 3-Kinase

PKA: Protein Kinase A

PVDF: Polyvinylidene Difluoride

RCC : Renal Cell Carcinoma

RISC: RNA Induced Silencing Complex

RNA: Ribonucleic Acid

RNAi: Ribonucleic Acid interference

RTK: Receptor Tyrosine Kinase

SDS-PAGE: Sodium Dodecyl Sulfate Polyacrylamide Gel Electrophoresis

shRNA: short hairpin Ribonucleic Acid

siRNA: small interfering Ribonucleic Acid

STR: Short Tandem Repeat

TBST: Tris-Buffered Saline with Tween20

thr: threonine

TLD: Thermoluminescent Dosimeter

TM: Transmembrane

UV: Ultra Violet

VEGF: Vascular Endothelial Growth Factor

VHL: Von Hippel-Lindau

1.0 Introduction

1.1 Background

1.1.1 Renal Cell Carcinoma

Renal cell carcinoma (RCC) represents 80% of cancers arising in the kidneys and 1–3% of visceral (soft organ) cancers [1]. RCC is thought to arise from the epithelial cells of the proximal convoluted tubules (see Fig. 1) which filter and collect waste products from the blood. Kidney cancers are generally divided into two major types. The remaining 20% are transitional cell carcinoma, which arises in the transitional epithelium (cells lining tubules of the kidneys and bladder).

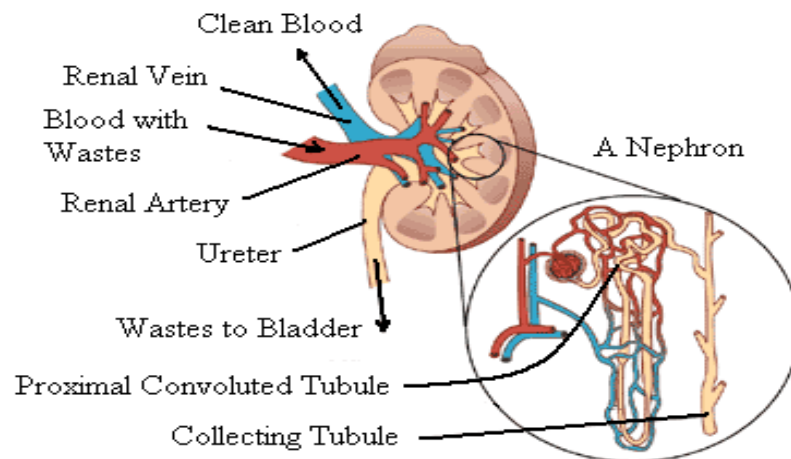


Fig. 1. Anatomy of a normal kidney. Blood enters the kidney through the renal artery and is passed over the nephrons in small capillaries. Waste products such as ammonia and urea are collected out of the blood here and into the convoluted tubules of the nephron. The waste products pass into the collecting tubules and into the ureter, destined for the bladder while filtered blood leaves through the renal vein. Renal cell carcinoma is thought to arise in the proximal convoluted tubules [1]. Image adapted from [2].

Worldwide, the incidence of RCC is highest in North America with approximately 15 cases per 100,000 people, with rates typically twice as high in males. Annually, 200,000 people are diagnosed with the disease worldwide [1]. The incidence of the disease is continually rising between 2–4% per year in Western countries with smoking as the largest known risk factor, followed by obesity and hypertension [3]. Inherited mutations may predispose an individual to developing RCC, most commonly a non- or poorly functioning VHL (Von Hippel-Lindau) protein. Such familial mutations are identified in about 4% of cases [4]. Typical symptoms of RCC include side pain, hematuria—blood in urine—and regional swelling in the abdomen [5]. Ultrasound is the most common diagnostic tool for detection of RCC, followed by a CT (Computerized Tomography) scan or MRI (Magnetic Resonance Imaging) [6], [7]. Early diagnosis of RCC is problematic as forty percent of cases display none of the main symptoms [8]. This frequent absence of symptoms is problematic as the disease often progresses unnoticed and will often metastasize—spread—to other organs, causing further complications. Indeed, 25–30% of RCC patients have metastatic tumours at diagnosis, and 70% will have metastatic tumours at some point during the course of the disease. The five-year survival rate of RCC is bleak at only 5–15% [1].

RCC is further divided into sub-types based largely on the observed morphology of cells when imaged with microscopy and histological staining. Chromophobe renal cell carcinoma occurs in ~5% of cases, and is less biased towards affecting males than other types. Tumours have a median diameter of six cm, making them typically the largest of the types of RCC. Survival is 83.9% at five years on average. Microscopically, cells appear large and polygonal with clearly-defined membranes and irregular nuclei [9].

Papillary renal cell carcinoma is found in 10–15% of RCC cases, 75% of which occur in men. The survival prognosis is similar to chromophobe RCC at 80–90% after five years. Papillary RCC takes its name from the circular, capsule-like structures that such tumours form microscopically [10]. This sub-type is considered less aggressive than other types and is often only found upon autopsy when the patient has died from another cause.

The most common sub-type of RCC is clear cell renal cell carcinoma (CCRCC), so-called because the cytoplasm stains clear with the common hematoxylin and eosin (H&E) stain. Cells typically grow in a sheet pattern, but can also take a tubular or papillary shape *in vivo*. CCRCC accounts for the majority, at 80% of RCC cases. It is considered a more aggressive and invasive sub-type that grows quickly, often outpacing the growth of blood vessels, despite possessing more vascularity than other types. Poor vasculature and oxygen supply (hypoxia) leads to necrotic centers in 10–15% of such tumours in which cells have died from lack of oxygen. Prognosis of CCRCC is the poorest of the subtypes with a five-year survival below 20% [11].

1.1.2 RCC treatment and radiation sensitivity

Radiation therapy is prescribed for about two thirds of all cancer patients at some point during their illness [1]. This type of treatment has been used since the early 1900s due to the ability of radiation to control tumour growth and kill tissue. Radiation therapy is a popular treatment option as it is generally less invasive than surgery and provokes less severe side effects than chemotherapy. Some types of blood cancers such as leukemia and lymphoma are particularly responsive and sensitive to radiation along with cancers of the germ cells. Most other cancers are moderately responsive to radiation and require a

special targeting procedure and multiple treatments to avoid delivering lethal doses of radiation to surrounding healthy tissue.

Treatment of RCC is usually limited to surgical removal of part or of the whole kidney (nephrectomy). Tumour ablation by burning or freezing, and immunotherapy are also employed, though nephrectomy remains most effective, despite risks of decreased kidney function and infection. Radiation therapy has typically been excluded from treatment of RCC as kidney damage was shown in the 1970s to be a common presentation for patients undergoing the treatment [12]. It was assumed that kidney tissue was therefore sensitive, until it was shown that most of this damage was caused only in conjunction with chemotherapy drugs, particularly Actinomycin, a transcription inhibitor [12]. The kidney's radiation sensitivity has been reclassified as only a moderately sensitive tissue with acceptable dose tolerance of 2.3 Gy [13]. Damage to healthy tissue aside, radiation therapy's effectiveness for RCC remains limited by the disease's resistance to radiation and chemotherapy, which are typically only employed for palliative care. Particularly, radiotherapy is used to reduce the pain caused by metastatic tumours in the bone and lower the risk of fractures [7]. Primary RCC tumours display resistance to traditional chemotherapy, whose slightly basic drugs are believed to be neutralized by the acidic local tumour environment. Recently, drugs targeting the VEGF growth receptor such as bevacizumab [14] have been employed to slow the progression of metastatic RCC, but to limited effect. Small molecule inhibitors such as pazopanib [15], sorafenib [16] and sunitinib [17] are also somewhat effective at stalling growth and spread of the disease by inhibiting tyrosine kinases. However, the response rate of these drugs can be as low as 10% of patients and disease resistance develops within

approximately 11 months for nearly all patients [18]. There is some indication that next generation drugs such as Axitinib [19] may be successful at improving chemotherapy for RCC, also by VEGFR targeting, however it remains largely unused.

Developments in radiotherapy technique, namely the introduction of robotic technology has resulted in the ability to target tumours with far more precision. The Accuray Cyberknife in particular allows the production of pencil-thin beams in nearly every conceivable angle, allowing the sparing of surrounding tissues. Since trials began in 1999, the device has been shown to provide superior growth control for metastatic RCC [20]. The same cannot be said of primary RCC tumours however as their resistance to radiation is difficult to overcome. Questions have also been raised concerning the machine's tendency to create radiation-induced secondary malignancies in patients [21].

As a result of radiation resistance, RCC tumours cannot be treated with radiation therapy without significant damage done to surrounding tissues. Thus the benefits of this non-invasive and low risk approach are not available to patients with RCC. As normal kidney tissue is relatively sensitive to radiation as opposed to the tumours that develop [22], it is believed that either genetic/proteomic or environmental changes occur in the process of transformation into RCC that renders the disease resistant to the effects of ionizing radiation. These transformative changes remain unclear.

1.1.3 Cell death by radiation and modes of resistance

Living cells are adversely affected by ionizing radiation. Radiation is ionizing when particles contain sufficient energy to liberate an electron from an atom, changing its charge hence ionizing it. Photons in the visible spectrum of light and of longer wavelength such as radio waves and infrared do not carry sufficient energy to ionize

atoms and upon colliding with other matter such as proteins or DNA, cause no immediate damage to their chemical bonds. However, photons with greater energy, such as UV- or X-rays will deposit this energy upon collision by ionizing cellular components, causing chemical bonds to break and/or reform improperly [23]. As the cell can usually produce more fats or proteins if they are damaged, collisions with these macromolecules are believed non-lethal. However, collisions with DNA pose much more of danger for cells as their proteomic expression and general functioning are dependent on the DNA being intact and having the correct sequence. While cells have the capacity to repair DNA, a certain threshold of damage will often trigger apoptosis [24], [25]. Alternatively, if the cell is actively dividing, a mitotic catastrophe may occur [26] in which DNA damage causes improper chromosome segregation and the resulting daughter cells are not viable. As a result, cells in G2 phase immediately before mitosis tend to be more sensitive to radiation insults, while cells in S phase are least sensitive due to the presence of DNA replication and repair machinery. Cells in senescence or dividing slowly such as neurons or muscle cells also tend to be resistant due to the decreased likelihood of entering mitosis with DNA damage. Cells in quickly dividing tissue such as bone marrow and jejunum crypt cells tend to be more sensitive, entering mitosis quickly with damaged DNA, resulting in mitotic catastrophe [26]. It is also worth noting that if the DNA of a cell is concurrently sustaining damage from other insults such as extreme temperature or intracellular pH, resistance to radiation is lowered. The cell's repair pathway responds to DNA damage regardless of cause and has a capacity can be overwhelmed [27].

It is unsurprising—given radiation damage to living cells is problematic due to DNA damage—that cells with reduced capacity to sense and repair this damage are more

sensitive to it. If mutations or aberrant expression occur in genes that perform these functions, radiation tolerance can be lessened, sometimes quite severely. Tumour suppressor genes such as p21 and p53 are often referred to as checkpoint genes as they arrest the progression of the cell cycle if conditions are not appropriate, including if the DNA has significant damage [28]. If they do not respond properly to DNA damage or fail to activate repair pathways, the cell can proceed through replication and mitosis with mutations or chromosome abnormalities that prove fatal via mitotic catastrophe. Ataxia telangiectasia is a recessive disease that occurs when the ATM (Ataxia Telangiectasia Mutated) protein cannot be recruited to double-stranded DNA breaks [29]. The defective protein fails to activate p53 and other tumour suppressors and stall the cell cycle for repair. Individuals with this mutation are incredibly sensitive to radiation and experience adverse reactions to even low-dose medical X-rays as their cells attempt to divide with severe DNA damage [30]. Proteins directly involved in repair pathways can also lose proper function or regulation. For example, mutations in the nucleotide excision repair pathway have been shown to increase radiation sensitivity. The pathway normally excises smaller point mutations in the DNA such as improper base-pairing or crosslinks between bases. Individuals with loss-of-function mutations in any of the eight genes involved may develop xeroderma pigmentosum. Individuals with this disease are hypersensitive to UV radiation due to its tendency to cause crosslinks between adjacent thymine residues, and must make every effort to avoid sun exposure [31].

There are two mechanisms by which radiation is believed to damage DNA, directly or indirectly. Direct damage occurs when a particle of ionizing radiation deposits energy into DNA itself, causing chemical bond reorganization. Indirect damage occurs

when energy is deposited into water molecules, often resulting in unstable free radicals which then donate or accept electrons inappropriately to DNA [32]. Direct damage is typical of large or charged particle radiation such as alpha particles, beta particles and neutrons. As they move through tissue, such particles deposit large amounts of energy in events that are close together, and are thusly consider high-LET radiation (Linear Energy Transfer). This proximity of ionizing events increases the likelihood that DNA strands are hit multiple times in the same location—such as once on each phosphate-sugar backbone—which results in double-stranded breaks that are more difficult to repair. By contrast, small and uncharged photons deposit small amounts of energy in events that are farther apart (low-LET). As energy disposition is spread farther apart, direct damage is less pronounced and results in mostly single-strand breaks [33] that are more easily repaired. It is believed therefore that photons contribute to DNA damage indirectly by ionizing water molecules. These ionized water molecules then interact with oxygen to create reactive oxygen species and free radicals which are believed to damage DNA themselves [34].

1.1.4 Radiation resistance and hypoxia

The model of direct and indirect damage implies that the presence of oxygen is important for the killing action of ionizing radiation. Moreover the presence or absence of oxygen is more important for photonic, low-LET radiation than other types [35], as the damage done to DNA is largely (approximately two-thirds) through oxygen radical intermediates. Experiments involving hypoxic or low oxygen levels consistently show that a minimum level of oxygenation greatly improves the killing power of photonic radiation such as X-rays. Cells that are hypoxic however, demonstrate greater resistance

to radiation. Schack and Macduffee irradiated mice with an eight Gy dose of X-rays. They found that mice that had been previously exposed to long periods of hypoxia by oxygen deprivation lost less bone marrow tissue and recovered it faster than control mice not exposed to hypoxia [36]. This effect is particularly problematic as most clinical radiation treatment machines deliver doses of photonic, X-ray radiation and therefore require tumours to be well oxygenated to be effective.

1.1.5 RCC and hypoxia

It is common for tumours to outpace the surrounding tissue's ability to provide sufficient blood flow to the area. This can significantly impede the tumour's growth progress as cells over approximately 120nm from a blood vessel will not receive sufficient oxygen. Grimbone et al. showed that the same tumour cells grow differently depending on available vascularization. Brown-Pierce carcinoma grafted into the iris of rabbits was able to vascularize and grow exponentially, yet when injected into the eye's anterior chamber, could not vascularize and eventually became dormant [37]. Furthermore, the tumour's growth outpacing angiogenesis—the creation of new blood vessels—can often lead to low-oxygen or hypoxic regions in the tumour [38]. This lack of oxygen can be extreme enough to be lethal for tumour cells in that area, causing the formation of necrotic sections. For example, Tannock found that mammary adenocarcinoma transplanted into mice displayed this particular pattern. Upon histological inspection of the tumours' arrangements, it was found that there were large pockets of necrotic cells, with only cylindrical strands of viable tumour cells running through them. These strands each contained a blood vessel, able to supply only the cells in close proximity [39]. As large parts of RCC tumours are found to be hypoxic as well, it

has been forwarded as a possible explanation of the radio-resistance seen in RCC. The hypoxia discourages indirect DNA damage as there is little oxygen available to form free radicals. This hypothesis is supported by the fact that the hypoxic response pathway is found activated in most RCC tumours via mutations in the VHL (Von Hippel-Lindau) gene [7] which normally suppresses this pathway. As a result, genes that allow cells to cope with hypoxic conditions are up-regulated and the tumour survives whilst being resistant to both oxygen deprivation and radiation.

1.1.6 Expression of carbonic anhydrase 9 as promoter of radiation resistance in RCC

Hypoxia discouraging indirect damage is not likely a complete explanation of RCC's radio-resistance as RCC lines *in vitro* under normoxic conditions still display poor sensitivity to radiation. We hypothesize that a downstream product of the activated hypoxia pathway may be responsible for this resistance, namely carbonic anhydrase 9 (CA9 or CA IX). CA9 is an appealing suspect as it is present in the majority of RCC (in over 95% of CCRCC) [40]. Its relationship as a downstream product of hypoxia is well established and it is considered a relatively accurate marker of hypoxia. Its usefulness as a prognostic factor is less clear however and is disputed [41]. While previously thought to merely catalyze the dissolution of CO₂, it has been found to encourage growth [42], invasion [42] and metastasis [43] in other tumour types, believed to be a result of increased acidification of the extracellular environment. In breast cancer cell lines which express CA9, the enzyme can be disrupted by inhibitors such as acetazolamide or RNA interference. Upon doing so, Robertson et al. observed that a lesser percentage of cells could migrate through porous membranes and matrixes. Moreover, bladder cancer cells not expressing CA9 were transfected with a constitutively active version of CA9

experienced an increase in their migratory and invasive capacity [42]. Though the authors conclude that CA9 is not solely responsible for migratory capacity, it is clear that the functioning of carbonic anhydrase 9 is not as simple as originally postulated. As we describe here, radiation resistance in RCC may be an additional effect of the enzyme that has previously been overlooked.

1.1.7 Carbonic anhydrases

Carbonic anhydrases (CAs) are enzymes which act as catalysts for the dissolving of CO₂ in water as carbonic acid and protons. This reversible reaction which proceeds relatively slowly by itself [44] can be increased to rate of around four–six million conversions per second in the presence of a single carbonic anhydrase molecule [45], making it amongst the fastest enzymes known. CAs typically feature a zinc (II) or sometimes cobalt (II) ion in the active site and are therefore considered metalloenzymes.

Carbonic anhydrases are divided into five families (α , β , γ , δ and ζ), believed to be the result of convergent evolution due to lack of homology in their genetic sequence. However, within these families, the amount of genetic and protein sequence homology suggests strongly that the various isozymes are related by common ancestry [46]. The α family is found in most organisms with the exception of archaea, and is the family of most importance to humans and other animals [47]. β CAs are found in archaea, bacteria, fungi, and algae and are common in plants. Varieties of γ CAs are found in prokaryotes and in both archaea and bacteria [48]. The last two families which have been identified are disputed due to similarities with the others. Diatoms produce the δ and ζ families, but δ CAs have been found to be similar at the active site to the α -types [49] and the ζ family shows structural similarity to the β family.

In mammals, family α is host to at least 15 isozymes which are sorted into 4 categories based on their localization. Carbonic anhydrases I, II, III, VII and XIII are cytosolic, IV, IX, XII and XIV are membrane associated, CAs VA and VB are mitochondrial and CA VI is secreted in milk and saliva [50]. CA isoforms perform critical functions throughout the body including facilitating respiration, pH buffering, bone resorption, the secretion of electrolytes, calcification and ensuring a sufficient bicarbonate supply for glucose, lipid and urea production [51]. CAs VII, X and XI are cytosolic and acatalytic; their function is unknown [52]. These proteins are also referred to as CARPs (Carbonic Anhydrase-Related Proteins).

1.1.8 Carbonic anhydrase 9: structure

Carbonic Anhydrase 9 (CA-IX or CA9) is the largest (459 amino acids) [53] of the mammalian CAs (54–58 kDa), and has unique domains that are not shared by its isozymes. The crystal structure (Fig. 2) has recently been solved [54], a process complicated by the enzyme's transmembrane nature. The extracellular domain features a signal peptide which likely localizes the enzyme to the membrane, a compact, globular catalytic domain similar to other CAs and a PG domain named as such because of sequences similar to proteoglycans. The PG domain sits above the active site and is thought to moderate interactions with other cells but also populate the active site with acidic amino acids as CA9 is most efficient at a slightly acidic pH [55]. Thus the production of acid by the enzyme by dissolving CO_2 creates a local environment where it can operate efficiently. The membrane is spanned by a single helix followed by a short intracellular tail [53]. The crystal structure also revealed CA9's tendency to self-dimerize, enforced by a disulfide bridge at cys⁴⁰⁹. In this state, both active sites are open to the

extracellular space and the PG domains are free to interact with nearby cells or the catalytic sites [54]. The presence of the intracytosolic tail domain is important for CA9's regulation. PKA (cAMP-dependent protein kinase A) can bind to the tail and phosphorylate CA9 at thr⁴⁴³. The phosphorylated form of CA9 is then capable of acidification; the non-phosphorylated version has greatly reduced enzymatic capacity. Moreover, in this form, the enzyme co-localizes with the bicarbonate importing metabolon NBC1 [56]. As CA9 produces bicarbonate, this localization with NCB1 may improve the efficiency of importation. This may allow tumour cells to maintain a higher internal pH despite an increasingly acidic extracellular environment.

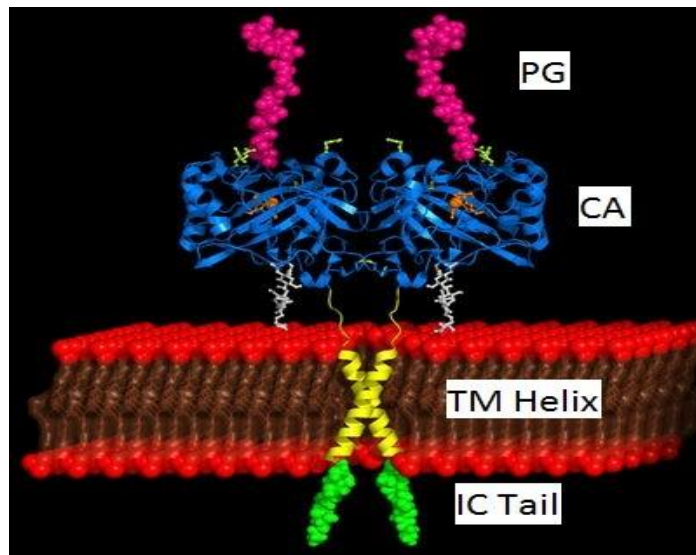


Fig. 2. A 3D model of a carbonic anhydrase 9 dimer in a phospholipid bilayer. From the N-terminus, the proteoglycan-like (PG) domain, catalytic carbonic anhydrase (CA) domain, the transmembrane (TM) helix and the intracytosolic (IC) tail. Adapted from [57].

Carbonic Anhydrase 9 exists in an alternatively spliced form that lacks the 8th and 9th exons. This splice variant creates a frameshift and premature stop codon in the transcript, resulting in truncation. The final protein product lacks a large part of the C-terminal region including the tail region, the transmembrane helix, cys⁴⁰⁹ which forms the intermolecular disulphide bridge and part of the catalytic domain. This form—54 as opposed to 58 kDa—does not seem to be as active, may be secreted to some extent and is present in small amounts in both normal and cancer tissues [58].

1.1.9 Carbonic anhydrase 9: expression and regulation

CA9 is expressed moderately in the gut lining [59] and in small quantities in the stomach and body cavity lining, but is otherwise not expressed in normal tissue. The enzyme is highly expressed under conditions of hypoxia [60] and is upregulated by HIF-1 α (Hypoxia Inducible Factor). Mutations in the tumour suppressor VHL gene (Von Hippel-Lindau) lead to stabilization of HIF-1 α which in turn causes the overexpression of CA9. VHL mutations are found in 22-57% of clear cell renal cell carcinomas [61]. Cell density has also been shown to encourage CA9 expression in HeLa cells, a phenomenon now believed to be caused by poor local oxygenation [62].

Carbonic anhydrase 9 is found expressed in many cancers due to its role as a downstream product of the hypoxic pathway. Because of relatively quick growth outpacing angiogenesis, tumours often experience hypoxic regions in which blood flow is not able to provide enough oxygen and remove carbon dioxide [63]. It is therefore advantageous for tumours to use CAs to dissolve excess carbon dioxide into water as bicarbonate rather than using limited amounts of binding sites on hemoglobin molecules to dispose of it. Moreover, it has been shown that the excess bicarbonate can be imported

into the cell to stabilize the pH of the intracellular environment and is used in the synthesis of pyrimidine nucleotides [64]. This is also believed to be the reason why the enzyme associates directly with the bicarbonate importing metabolic NBC1.

Under normoxic conditions, CA9's transcription factor HIF-1 α (Hypoxia Inducible Factor) is hydroxylated at Pro⁵⁶⁴ by PHD (prolyl-4-hydroxylase) [65]. This allows ubiquitylation to occur with the aid of the von Hippel-Lindau protein (VHL) [66], along with eventual proteasome degradation. The end result is that HIF-1 α does not remain intact long enough for it to carry out significant transcriptional promotion. However, PHD requires dioxygen to function and when a cell becomes hypoxic, HIF-1 α does not become hydroxylated and does not interact with VHL or undergo degradation. Instead, the protein remains stable and enters the nucleus, dimerizing with HIF- β to form a functional transcription factor HIF which allows transcription of CA9. The dimer recognizes sequences called hypoxia response elements (HREs) which are found in genes responsible for angiogenesis such as vascular endothelial growth factor (VEGF), glucose transporters and other genes related to survival and proliferation [67]. This relationship with hypoxia means CA9 may be a useful marker for the condition as well as a predictor for therapeutic outcome in radiation and chemotherapy [68]. Mutations in the tumour suppressor VHL gene can also lead to constitutive expression of the hypoxic response including CA9 which can be found expressed up to 150-fold the normal level [69].

1.1.10 Carbonic anhydrase 9: other known functions in tumours

The presence of carbonic anhydrase 9 on the surface of tumour cells is believed to contribute to the acidification of the local tumour environment. Due to its dissolution reaction being reversible, CA9 also guards tumour cells against the danger of acidosis.

Hypoxic tumours often are found to have a pH of about 6 as opposed to the physiological normal of pH 7.4. The presence of the PG (Proteoglycan-Like) domain is believed to make the enzyme function efficiently at acidic pH levels. CA9's catalytic subunit has a pKa around neutral, while the presence of the PG domain lowers it to 6.5 [54]. Inhibition of the active site leads to an increase of pH in cellular media. This effect can be replicated by the deletion of the catalytic subunit, demonstrating the contribution of CA9 to acidification by the generation of carbonic acid in addition to the lactic acid produced by anaerobic respiration [70]. In turn, a low pH has been linked to increased invasion, migration, expression of growth factors, chromosome rearrangements and breakdown of the extracellular matrix by proteases such as matrix metalloprotease 9 (MMP-9) [71]. CA9 may also contribute to migratory potential in tumours cells by interfering with anchoring proteins. MDCK cells transfected with CA9 constitutively show weaker adherence ability. Co-immunoprecipitation showed CA9 bound with both E-cadherin and its cytoskeletal intermediate β -catenin. This suggests competition for, or interference with adherens junctions [72] which may in turn allow loose adherence and greater migratory ability for cells expressing CA9. Conversely, fibrosarcoma cells transfected with silencing RNA targeting CA9, lost migratory capacity and developed a stronger adhesive capacity [73].

In addition to pH regulation and cellular mobility, there is some evidence that points to carbonic anhydrase 9 having a role in cell signaling. Structurally speaking, it is peculiar that the enzyme should dimerize as its kinetic and enzymatic properties do not depend on it. It has been noticed also that many CARPs (carbonic anhydrase associated proteins) are tyrosine receptor kinases (RTKs) which share CA9's catalytic domain [52].

Although the domain is non-catalytic in these cases, RTKs are known to be heavily involved in pro-growth signaling, meaning that it may have signaling function in CA9 as well. To this effect, Dorai et al. exposed SKRC-01 human RCC cells to increasing amounts of the pro-growth ligand EGF (epidermal growth factor). Using immunoprecipitation, it was shown that EGF stimulation results in phosphorylated tyrosine residues on CA9, though the mechanism by which this occurs is unknown [74]. This demonstrated that CA9 is involved in EGF signaling, either directly or indirectly through EGFR (EGF-receptor). Further co-immunoprecipitation revealed that the phosphorylated tyrosine allowed CA9 to interact with PI3K (phosphatidylinositol-3 kinase). Dorai et al. also demonstrated that the CA9-PI3K complex could phosphorylate—and therefore activate—the protein AKT. AKT in turn is a known activator of the mTOR (mammalian target of rapamycin) pathway which over-actively suppresses apoptosis. When CA9 was not present in significant amounts to act as an intermediate, this EGF activation of AKT did not occur [74]. In short, CA9's presence in RCC may enable suppression of the apoptotic pathway (see Fig. 3 for summary). If this is true, cells expressing CA9 may not self-terminate after significant radiation damage. CA9's possible role as a suppressor of apoptosis is therefore perhaps the strongest reason to suspect its involvement in the radiation resistance of RCC which express it.

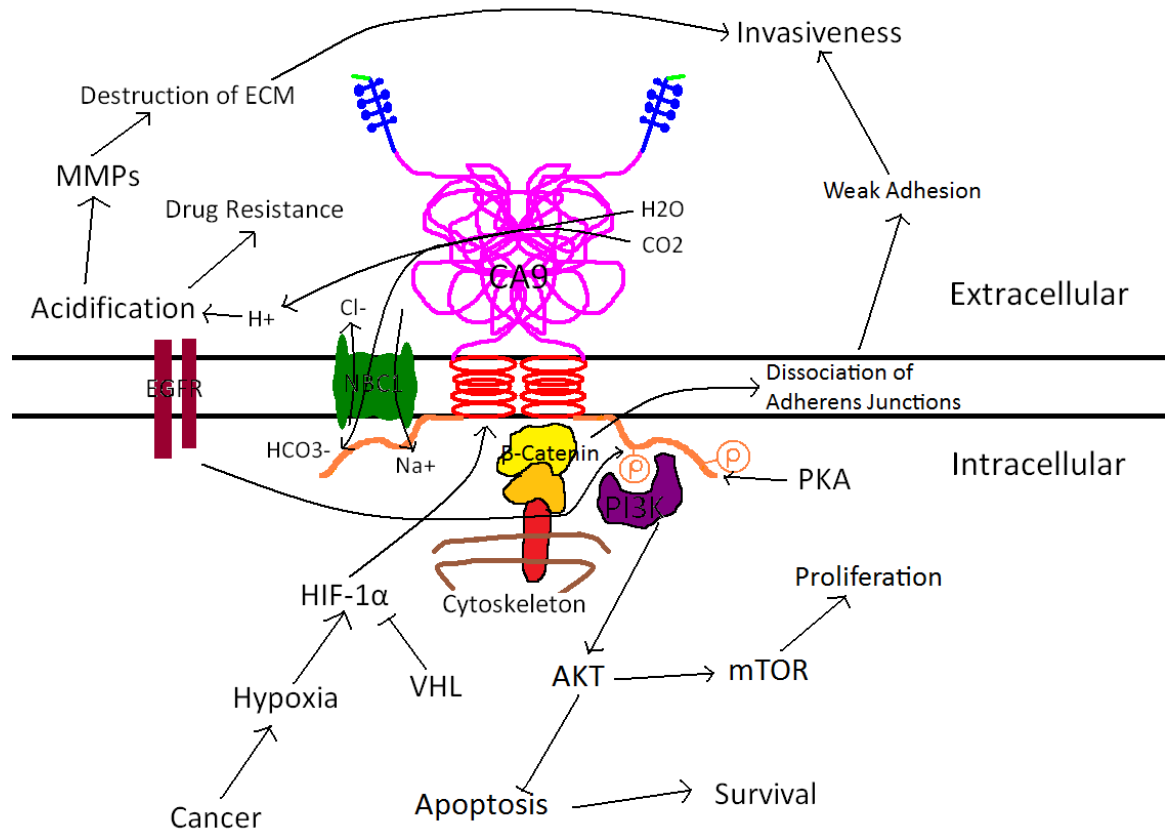


Fig. 3. Summary of upstream effects on, and downstream effects of CA9. Hypoxia from rapid tissue growth allows the stabilization of HIF-1 α which can also be caused by mutations in the negative regulator VHL. HIF-1 α allows the transcription of CA9 which may self-dimerize and requires PKA to phosphorylate a tail threonine residue to perform catalysis. CA9 produces bicarbonate which is imported by NBC1 and protons which acidify the extracellular space. The acidic environment neutralizes weakly basic drugs and activates MMPs which degrade the extracellular matrix allowing further invasion. CA9 competes with cadherins for β -catenin binding sites and prevents normal adherens junctions from forming, weakening cell adhesion. EGFR stimulation phosphorylates tyrosine residues on CA9 which recruits PI3K and activates AKT, leading to the suppression of apoptosis and activation of the pro-growth mTOR pathway.

1.2 Approach

1.2.1 Targeting carbonic anhydrase 9

One possible method of determining CA9's role in the radio-resistance of RCC is to inhibit the function of the enzyme and to measure any resulting change in cells' ability to survive radiation insults. Here, two methods are used to inhibit CA9's functionality. One approach involves targeting the enzyme with the drug AEBS (4-(2-aminoethyl)benzene sulfonamide). AEBS is a small molecule which has in drug screening tests been demonstrated as an efficient inhibitor of the enzymatic activity of CA9 [75] by competition for the active site. It also displays specificity for CA9, which is rare as the various isozymes of CA have very similarly structured active sites. It should be noted however, that the drug also efficiently inhibits isozyme CA12 (Ki 10-fold lower) [75], which is membrane-associated as well. Sulfonamides, as the name suggests, contain a sulfonamide functional group—a sulfonyl group connected to an amine group (SO_2NH_2). Similar sulfonamides were used as anti-bacterial agents before the discovery of antibiotics and are used today to mediate water transport and pressure in various parts of the body [76]. They may function as diuretics and can relieve ocular hypertension—doing so by inhibiting carbonic anhydrases no less. Though they usually are associated with very few side-effects, they occasionally provoke severe allergic reactions [76]. One study which used a similar sulfonamide, acetazolamide, demonstrated its inhibitory capacity of CA9 in clear cell carcinoma line 786-O, and concluded that the inhibition encouraged apoptosis [77]. This lends credence to CA9 being necessary for radiation tolerance; if inhibition encourages apoptosis, then this may limit a cell's ability to avoid apoptosis after a radiation insult.

Alternatively, RNAi (RNA Interference) may be used to target CA9's transcript, preventing it from being expressed. RNAi is an important regulatory mechanism which is both critical to early-life growth and development as well as defense against retro-viruses. The enzyme Dicer [78] detects and cleaves double-stranded RNA (dsRNA) into small fragments of ~20 bp. One strand is degraded and the other is taken up by an enzyme complex known as RISC (RNA Induced Silencing Complex) [79]. While in the complex, the small RNA (now a siRNA or Small Interfering RNA) may base-pair with a complementary sequence such as an mRNA. When this occurs, the RISC complex cleaves the paired strand which is eventually degraded, preventing the transcript from being translated and the protein expressed. Cells encode and produce their own siRNAs called miRNAs (Micro RNA) to downregulate genes. MiRNA are transcribed from open reading frames and base-pair with themselves [80] in a particular hairpin conformation. This double-stranded conformation is recognized by cell machinery and processed into a siRNA. Dicer cleaves dsRNA from viruses as well however, and uses the resulting siRNA to target other viral RNA for degradation as a defense mechanism [81].

This pathway can be exploited as a biomedical tool to downregulate genes of interest [82]. Exogenous siRNA can be added in a pre-cleaved form or by introducing an open reading frame which transcribes a hairpin RNA similar to miRNA. It becomes similarly processed and downregulates the gene of interest in a semi-permanent fashion assuming the opening reading frame can be introduced via stable transfection of the cells of interest. Fortunately, vector plasmids carrying such reading frames can be introduced to cells which sense the DNA fragments and attempt to repair the perceived damage by incorporation of the fragment into the genome. This process is not completely

understood, but can be aided with electroporation, calcium phosphate and various cationic lipids or complexes. In this fashion a RCC line can be made to produce significantly less CA9, allowing radio-sensitivity testing when the enzyme is mostly absent rather than merely inhibited.

1.2.2 Measuring radiation resistance of RCC

A standard method of measuring radiation resistance of cells *in vitro* is the clonogenic assay [83]. Clonogenicity refers to the ability of a single cell to grow and divide to form a descendant colony or clone. Generally, cells are seeded as a single cell population, subjected to an insult and then allowed to grow. After a growth period, the surviving cells will grow into colonies. If for example, the insult killed 30% of the cells, only 70% of expected colonies will form. The expected number of colonies is determined by a control population that was not subjected to the treatment. When the surviving percentage or fraction is plotted against each degree of insult (for example radiation dose) a survival curve is created. This is the standard format for comparing radiation sensitivity between cell types at least *in vitro* [84]. It should be noted that failure to form a colony within the time period does not necessarily mean the cell in question is dead; it may be merely unable to reproduce or reproduce very slowly. However, as the goal of cancer treatment is often to prevent the growth and spread of the disease and not always necessarily to eradicate it entirely, this endpoint of inhibited growth is generally accepted as sufficient.

1.2.3 Cell lines considered

The 786-O human clear cell renal cell carcinoma line is characterized by a VHL mutation and a lack of wild type protein product. Re-introduction of wild-type VHL does

not affect the growth of the line *in vitro*, but does prevent the cells from forming tumours in nude mice [85], [86]. CA9 expression, which has been detected in 786-O cells, can also be reduced by this re-introduction of VHL [86]. Curiously, the cells lack normal HIF-1 α however, pointing to the possibility of alternative regulation and promotion of CA9 expression. Another isoform, HIF-2 α , has been shown to be functionally dominant in this line, providing a possible explanation for CA9 expression. This isoform has been shown to regulate VEGF, which is another downstream product of the hypoxic HIF pathway [87]. Like CA9, the VEGF promoter sequence has a HRE (Hypoxia Responsive Element), which is recognized by the HIF complex and can do so regardless of which version of the α subunit is present. Although not yet shown, it is possible that CA9's promoter sequence may also be regulated by HIF-2 α . Experiments using these cells have also shown that the intracellular pH can be lowered and apoptosis activated by inhibition of CA9 with small molecule drugs [77].

The murine RAG line (renal adenocarcinoma) is uncharacterized in terms of hypoxic pathways. The line is studied mainly for its defective regulation of MHC II (Major Histocompatibility-Complex, Class II) genes [88]. Although such kidney cells are not involved in the immune response, the regulation of the antigen-binding MHC genes is frequently found to be disrupted in many cancer types, though it is unclear why. As a further curiosity, the RAG genome is thought to be unstable; cells display a great deal of heterogeneity in their chromosome arrangements and ploidy [89]. We have included it as a cross-species comparison of RCC.

Human LNCaP (prostate adenocarcinoma) cells have been shown to not express CA9 [90], and are thought to be radiation-resistant [91], [92]. Similarly to the 786-O line,

hypoxia-response pathways have been studied in LNCaP cells in detail. While adherent, the cells do not maintain a neat monolayer. As available, *in vitro* space becomes scarce at higher confluences, the cells begin to pile on top of each other. This ability to grow the cells in high density has been useful for studying localized hypoxia. Higher densities induce the hypoxic response in the LNCaP line as cells compete for the little oxygen available to them. HIF-induced expression of reporter genes with associated hypoxia response elements in their promoters can be up to 250-fold higher in densely seeded *in vitro* conditions for this reason [93]. We included the cells as a benchmark to make survival experiments comparable to other *in vitro* radiation survival experiments, and to test if results could be duplicated in non-RCC lines which do not express CA9.

Glioblastomas such as the human LN-18 cell line are considered to be amongst the most resistant cell lines to radiation insult [94]. The reason for this resistance is believed to be a constitutively active AKT pathway that actively suppresses apoptosis [95]. Curiously, CA9 is also found upregulated in LN-18[96], which as explained in section 1.1.10, may not be entirely coincidental. The cell line however, is included here only as a comparable benchmark for radio-sensitivity of RCC cell lines.

1.2.4 Xenografts

In vitro models of radiation resistance in tumours are limited in their approximation of tumour environment. Cell signals from surrounding tissues, physical constraint by the extracellular matrix, localized pH changes, blood circulation and hypoxia are not present in cell culture dishes. The results of *in vitro* experiments therefore may not extend to practical, clinical circumstances where these factors may or may not influence radiation resistance. To include these factors in a radiation resistance

experiment, xenografts are more useful approximations. Xenografts are tissue that has been transplanted from one species to the next. As such, human cancer cells or grafts may be injected or surgical implanted into mice to form tumours. Human tumours in mice are generally considered a far better approximation of the disease and are widely used [97]. One of the most common mouse strains for such experiments is the BALB/c, an inbred, albino type bred specifically for lab work [98].

1.2.5 Nude mice

Xenografting can be complicated by the host mouse's immune system which recognizes human antigens as foreign and may attempt to fight off the tumour cells that have been implanted. The tumour take rate—percentage of xenografts that grow successfully inside the host animal—is often less than 100% [99], necessitating the use of more transplanted tissue or host animals. Unsurprisingly, the rejection chance of the xenograft can be lowered if the host animal has a compromised immune system. The immune system of nude mice is largely comprised in this way, making this sub-strain of BALB/c mice ideal for xenografts. Nude mice contain a mutation in the sequence of the FOXP1 transcription factor. Mice with the mutation do not develop a thymus, meaning they cannot produce mature T-lymphocytes—a group of white blood cells involved in recognizing foreign antigens [100]. Nude mice therefore cannot recognize human cancer cells as well as their non-mutant counterparts, and make more practical xenograft hosts.

1.3 Hypothesis and objectives

1.3.1 Objectives

To determine if carbonic anhydrase 9 plays a role in the radiation resistance of renal cell carcinoma and if targeting the enzyme using inhibition or silencing RNA may improve the effectiveness of radiation therapy.

1.3.2 Hypothesis

Carbonic anhydrase 9 expressed in renal cell carcinoma confers radiation resistance to the cancer and downregulation or inhibition of CA9 sensitizes RCC to the effects of ionizing radiation.

2.0 Methods

2.1 Cell culture

786-O (human clear cell renal cell carcinoma), RAG (mouse renal adenocarcinoma), LNCaP (human prostate adenocarcinoma) and LN-18 (human glioblastoma) cell lines were purchased from ATCC. Medium used for all cell lines in all situations was RPMI-1640 (Hyclone) supplemented with 25.03 mM HEPES, 2.05 mM L-glutamine, 10% FBS (Invitrogen), 0.893 M sodium bicarbonate (Invitrogen), 1.0 mM sodium pyruvate (Invitrogen) and 0.0814 g/L MEM non-essential amino acid solution (Sigma). Cells were grown in either 10 cm polystyrene cell culture dishes (Corning) with 8 ml of medium or—during the process of creating stably transfected cell lines—in six-well polystyrene cell culture plates (Greiner Bio-One) with 3 ml/well of medium. Incubation occurred in a Thermo Forma Series II water jacketed, HEPA filtered incubator with 5% CO₂ at 37°C. Manipulation of the cells was performed in a Forma Scientific Class II A/B3 Biological Safety Cabinet. Cells were passaged upon reaching 90% confluence (unless otherwise stated) by aspirating medium, washing twice with PBS (Amresco), digesting for 10-15 min with 0.05% trypsin (Thermo Scientific), and reseeding into new dishes. For 10 cm dishes, 4 ml of PBS was used in each wash, 3 ml of 0.05% trypsin was used for digestion and for wells of six-well plates, one ml of PBS was used in each wash and one ml of 0.05% trypsin was used for digestion. In both cases a one in ten dilution of cells was reseeded into new vessels for the next passage. The authenticity of 786-O cells was verified by ATCC by STR analysis. For long-term storage, cells from 10 cm dishes were washed and subjected to trypsin digestion as described above, placed in a 15 ml polypropylene tube (Falcon) with eight ml of

supplemented medium and centrifuged at 300 g for seven min at room temperature in an IEC Centra-7X centrifuge. Supernatant was discarded, the pellet resuspended in 3 ml media per 10 cm dish containing 10% DMSO (Caledon) and one ml of the cell suspension aliquotted into one ml cryovials (Pathtech). Vials were kept for 24 hours at -80°C and were then moved to the gas phase of a liquid nitrogen tank until further use. For cell counting, 10 µl of cell suspension was added to a haemocytometer and the number of cells counted using a VWR hand tally counter.

2.2 Mycoplasma detection by DAPI (4',6-diamidino-2-phenylindole)

All cells in culture were screened once every two weeks for mycoplasma infection by DAPI (AAT Bioquest) staining. The medium from 10 cm dishes containing cells at 50% confluence was aspirated and the cells were washed twice with four ml PBS. Eight ml of a 0.5 µg/ml DAPI solution in 99.8% methanol (Caledon) were prepared in a 15 ml tube and added to each dish for five min at room temperature. The DAPI mixture was then aspirated and cells rinsed once with four ml of 99.8% methanol. Dishes were kept open until remaining methanol had evaporated. A DM IRB (Leica) fluorescence microscope with a 100 W mercury bulb (Chiu Technical) at 200x magnification was used to image the cells (λ emission = 470 nm, λ excitation = 350 nm). Cells were evaluated for mycoplasma infection according to the criteria mentioned in appendix B. The presence or absence of mycoplasma was confirmed by PCR amplification of mycoplasma specific DNA sequences from medium samples according to [101].

2.3 Transfection of 786-O cells

pGFP-V-RS plasmid vectors with four unique knockdown target shRNA sequences (see appendix C) for carbonic anhydrase 9 or non-effective scrambled control

shRNA were purchased from Origene and reconstituted in 50 μ l dH₂O to obtain a DNA concentration of 100 μ g/ml. 786-O cells were seeded in 6-well polystyrene plates (Greiner Bio-One) in three ml supplemented media per well and allowed to grow to confluence. Ten μ l plasmid solution (containing 1 μ g DNA) per well was added to the cells according to the retailer's instructions with 12% Fugene (Promega) as the transfection agent. Cells were screened at 24 and 72 hr post-transfection for green fluorescent protein (40x) with a fluorescent microscope at 510 nm (395 nm excitation). Protein lysates were created (see section 2.4) to assess knockdown by Western blotting.

Following the 72 hr transfection period, cells were passaged as previously described but with only a 1 in 100 dilution of suspension reseeded into a new well with media containing 1.0 μ g/ml puromycin as a selection agent as per manufacturer's instructions (Sigma). Puromycin was prepared as a 100x stock solution in dH₂O stored at -20°C and freshly added each media change or passage.

After one week of incubation, resulting colonies were screened again for green fluorescent protein using fluorescent microscopy. Positive colonies were marked with a permanent marker on the bottom side of the well. Media was aspirated and positive colonies were selected by gently scraping the colony with a pipette tip and stirring into fresh 1.0 μ g/ml puromycin-containing medium in a new well of a six-well plate. Four colonies were picked for each transfected plasmid type for a total of 16 potential stable cell lines with knocked down CA9 and four scrambled control subclones.

The 20 selected subclones were allowed to incubate for one more week in six-well plates, and upon colonies reaching a size of ~50 cells, selected again as previously described to ensure each cell line contained a homogenous population. Following the

second selection, cells were grown and passaged normally in six-well plates with medium containing 1.0 µg/ml puromycin for three weeks.

2.4 Preparation of protein lysates

Medium was aspirated from six-well plates or 10 cm dishes containing 100% confluent cells which were washed twice with one ml or four ml PBS, respectively. Plates or dishes were placed on ice and subjected to a lysis buffer of 0.0160 M Triton X-100 in PBS for 10 min. Dishes received 675 µl of buffer and six-well plates received 300 µl per well. “Halt” Protease Inhibitor Cocktail (Thermo Scientific) and Phosphatase Inhibitor Cocktail (Bioshop) were added to the lysis buffer in a 1/100 ratio. Cells were scraped from the dishes or wells using a rubber policeman into 1.5 ml microcentrifuge tubes (Diamed) and sonicated five times for one sec at 40 A using a Vibracell sonicator. Tubes were centrifuged using an Eppendorf Centrifuge 5415C at 2000 g for 10 min at room temperature and the supernatant was transferred to a fresh 1.5 ml tube and stored at -20°C until further use.

2.5 Determination of protein concentration

Protein concentrations of lysates were determined using the DC Protein Assay (BioRad) on a 96-well plate (Falcon) with a standard curve of bovine serum albumin ranging from 0.1 to 1.25 mg/ml. Cell lysates were thawed on ice and vortexed briefly. Five µl of lysate was added to 20, or 45 µl of PBS in microcentrifuge tubes to make 5- and 10- times dilutions respectively. Dilutions were then vortexed and five µl was pipetted into a well of a 96-well plate as per the manufacturers’ instructions. All three dilutions were run in duplicate. Colorimetric readings were taken on a Biotek Powerwave HT

spectrophotometer at 750 nm using the KC Junior program. The end concentrations of the 5- and 10-times diluted samples were averaged for each lysate.

2.6 Western blot analysis

Twenty μg of protein lysates were prepared in reducing loading buffer using 5 volumes of protein lysate and 1 volume of 6x loading buffer (0.35 M Tris pH 6.8, 0.35 M SDS, 4.1 M glycerol, 18 mM bromophenol blue, 0.6 M DTT). Samples to be run under non-reducing conditions were similarly prepared, with the omission of DTT from the loading buffer. Reduced samples were boiled at 100°C for 5 min prior to loading. The proteins were separated using a BioRad Powerpac Basic in 1.5 mm wide, 10% or 8% (bis)acrylamide (BioShop, 40:1 Bis) gel electrophoresis (see appendix A). Gels were run for one hr at 50 V and one hr at 100 V in running buffer (see appendix A) at room temperature. The proteins were transferred from the gel to PVDF membranes pre-soaked in methanol using wet electrophoretic transfer at 85 V for one hr on ice in transfer buffer (see appendix A). Membranes were blocked with 5% skim milk in TBST (0.015 M NaCl, 10 mM Tris pH=7.4, 45 mM Tween-20) for one hr. Antibody incubation occurred in glass containers on a Labnet Orbit LS at 60 rpm for two hr at room temperature (in primary antibody), or one hr (for secondary antibody). Incubation solutions of 2.5% skim milk in TBST with 1:1000 and 1:1000 dilutions of primary and secondary antibody respectively were used (see appendix for list of used antibodies). Super Signal West Pico Luminol and Stable Peroxide Solution (Thermo Scientific) were used to generate luminescence while exposed to Bioflex imaging film. Film was processed using a JP-33 X-ray film developer. Actin was used for normalization with Lab Image software to estimate the amount of

CA9 present by densitometry. Readings were multiplied by the densitometry ratio of actin in each lane to control for protein content.

2.7 Survival assays

Cells from 90% confluent 10 cm dishes were brought into suspension as mentioned in section 2.1. The cell suspension was added to eight ml of media and centrifuged at 300 g for seven min in an IEC Centra-7X centrifuge. All but two ml of supernatant was aspirated and the cells were resuspended by pipetting with a one ml pipette. The cell number was determined using a haemocytometer and the cell suspension was diluted to five cells/ μ l with media. For 786-O, RAG or LN-18 cells, 250 were seeded—per well—into 6-well plates (1000 cells in the case of LNCaP cells). 786-O and RAG cells were incubated at 37°C and 5% CO₂ for four hours to allow the cells to attach to the plate, while LNCaP and LN-18 cells incubated for 24 hr. At this point the cells underwent treatment, if any. Following the treatment, incubation continued for 6 days (786-O cells), 7 days (RAG cells), or 12 days (LNCaP and LN-18 cells) including attachment incubation and treatment time. Following incubation, the cells were washed twice with one ml PBS (per well of a six-well plate) and stained with a 0.25% crystal violet solution in 95% ethanol for 10 min at room temperature. Plates were then rinsed three times by submergence in tap water at room temperature and left to dry overnight. Using a ruler and scalpel, a six mm by six mm grid was etched into the bottom of the wells to aid counting. Colonies of 50 cells or more were counted using a Leica DM IL microscope and VWR hand tally counter. Plating efficiency controls—plates receiving no treatment—were included for every experiment. Counts of treated plates were compared to plating controls to obtain the fraction or percent surviving i.e. average count of treated

plates/average count of plating controls = fraction surviving treatment. Different concentrations of AEBS were added in 100 μ l of dH₂O to three ml media with final concentrations ranging from 3.3 μ M AEBS to 3300 μ M. An AEBS stock solution of 33 mM was prepared in H₂O, sterile-filtered using a Uniflo sterile syringe filter. IC₅₀ was calculated using the CalcuSyn [102] program's dose-effect curve generator.

2.8 *In vitro* irradiations

Irradiations of cells were performed using a Varian Linear Accelerator (LINAC) generating six MV X-rays. Cells plated in duplicate six-well plates were irradiated at a distance of 100 cm (source to well bottom) in a 16 cm by 20 cm field. A 19 mm-thick acrylamide sheet was placed on top of the plates to act as a build-up region.

Thermoluminescent dosimeters (TLDs) were used to measure and calibrate the dose delivered in the setup per monitor unit of the machine. Control plates (containing untreated control cells) accompanied experimental plates to the treatment area for mock irradiations and to account for the effects of additional movement and radiation scatter. Cells otherwise received from one to eight Gy in survival experiments. For fractionation survival assays, cells received irradiation with two Gy or a mock irradiation, repeated twice more 24 and 48 hr later for a total of three 2 Gy doses or mock doses.

2.9 Activity assay

Cells were seeded in six-well plates and allowed to grow to confluence. Media was aspirated and the cells were washed twice with one ml PBS per well. One ml of a solution of 0.9% saline (adjusted to pH 8.0 with NaOH) containing 0.15 mg/ml phenol red was added to each well. One hundred μ l of deionised water with or without AEBS at various concentrations was added to wells. Starting five sec after the addition of saline to

the cells, the absorbance at 565 nm was measured using a Biotek Powerwave HT spectrophotometer and corresponding KC Junior software at one sec intervals for 20 sec. The absorbance was measured in one well at a time to decrease the time between reads. Absorbance readings were exported from KC Junior to Microsoft Excel. The relative absorbance of a particular well throughout the 20 sec was determined as a percent of the no cell control average at that time interval ($A/A_{\text{no cells}}$).

2.10 *In vivo* resistance assay

2.10.1 Animal care and monitoring

Forty female BALB/c NU/NU (nude) mice were purchased from Charles River Laboratories at an age of 6 weeks upon arrival. This study was approved by McMaster University's Animal Research and Ethics Board (AUP# 12-09-37) and all experiments were performed in accordance with the board's requirements for animal usage. Mouse weight, tumour volume and condition was actively monitored as prescribed by the board. Animals were maintained by the McMaster University Central Animal Facility staff, provided constant access to food and water, and were kept with an alternating photoperiod of 12 hours of light/12 hours of darkness. Mice were given one week to acclimatize to the facility upon arrival before any handling or procedures were performed. Irradiations and mock irradiations occurred while mice were under gaseous isoflurane/oxygen anaesthesia. Mice were identified by small incisions made in the outer ear lobe.

2.10.2 Tumour xenografts

Nine 10 cm dishes containing 100% confluent shScr or shCA9 786-O cells were subjected to trypsin digestion as described in section 2.1. Cell suspensions were added to

10 ml of media in 50 ml tubes for neutralization. Cell concentration was determined by counting by haemocytometer. The cells were centrifuged at 300 g for seven min at room temperature in an IEC Centra-7X centrifuge. Supernatant was removed and cells were resuspended in media at a concentration of one million cells/100 µl, then diluted 1:1 with Matrigel (BD Biosciences). Two hundred µl was loaded slowly into 3 ml syringes with 27-gauge needles and kept on ice. The injection site on each animal was treated with an ethanol swab for disinfection and one million cells of either the shScr or ShCA9 sub-line was injected subcutaneously into the right flank (20 mice per group).

2.10.3 Animal irradiation

After solid tumours had formed twenty-one days post injection, animals were anaesthetized with a isoflurane/oxygen mix and positioned in sterile, acrylamide cylinders connected to a portable anaesthetic machine. Cylinders were taken four floors down to a treatment bunker, positioned at a distance of 100 cm to source and irradiated with six Gy in a two cm by two cm field using a Varian Linear Accelerator (LINAC) generating six MV X-rays. A five mm-thick sheet of superflab bolus material was employed as a build-up region. Animals in non-irradiated control groups were merely anaesthetized for a similar time period. Following irradiation or mock irradiation, animals were warmed by hand until consciousness was regained. In summary, the four treatment groups were i) an injection of shScr cells with radiation, ii) shScr cells mock-radiation, iii) shCA9 cells with radiation and iv) shCA9 cells mock-radiation.

2.10.4 Data collection

Tumour volume was measured periodically post-injection using callipers and recorded as a function of length by width by depth. At 87 days post-injection, animals

were euthanized by gaseous CO₂. Blood was collected immediately by cardiac puncture and after an hour at room temperature, was centrifuged using an Eppendorf Centrifuge 5415C at 2000 *g* for 20 min. Supernatant serum was frozen at -80°C. Tumours were surgically removed and weighed using a Mettler AE163 scale. Half of each tumour was placed in a cryovial and snap-frozen in liquid nitrogen to prepare homogenates for Western blot analysis. The other half was preserved in formalin for 30 hours and embedding in paraffin for histological examination by H&E staining.

2.11 Statistics

All error bars displayed in figures represent \pm standard error of the mean. Microsoft Excel's unpaired, two-tailed, Student T-Test assuming unequal variance of groups was used to perform significance testing for *in vitro* experiments. Due to low sample size, the non-parametric Mann-Whitney U test was employed for *in vivo* experiments. P values ≤ 0.05 were considered significant.

3.0 Results and Discussion

3.1 CA9 is present in 786-O, RAG and LNCaP cells, undetectable in HEK cells

As we hypothesize that CA9 confers radiation resistance, we first confirmed that the RCC cell lines to be used express CA9. Protein lysates of human prostate cancer LNCaP, human clear cell renal cell carcinoma 786-O, murine RCC RAG and immortalized human embryonic kidney HEK-293 cells were therefore analyzed by Western blot analysis for the presence of CA9 (Fig. 4). Using Epitomics antibody 3829-1, CA9 was detectable in LNCaP, 786-O and RAG cells, but not in HEK-293 cells.

This confirms a previous report of CA9 expressed in the 786-O cell line [77]. This is the first time to our knowledge that CA9 has been tested for and shown to be expressed in RAG cells, but as the cell line is derived from a renal cell carcinoma—many of which express CA9 [40], [41]—it is not surprising. However, the detection of CA9 in LNCaP cells contradicts previous reports that the cell line does not express the enzyme [90]. However, LNCaP cells are known to be hyper-sensitive to cell density and oxygen supply with respect to HIF-1 α 's expression which varies greatly depending on these conditions [93]. Moreover, the induction of the HRE (Hypoxia Responsive Element) increases 150–250 fold in this line when cells are seeded densely [93]. It may be that we have detected CA9 here merely because protein lysate samples were taken from dense, highly confluent cultures. HEK cells are immortalized cells derived from normal human embryonic kidney tissue, which does not normally express significant amounts of CA9 [103]. In Fig. 4, CA9 appears as two bands, the lower of which most likely represents the truncated, poorly understood, alternatively spliced isoform [58] (54 kDa, full variant is 58 kDa).

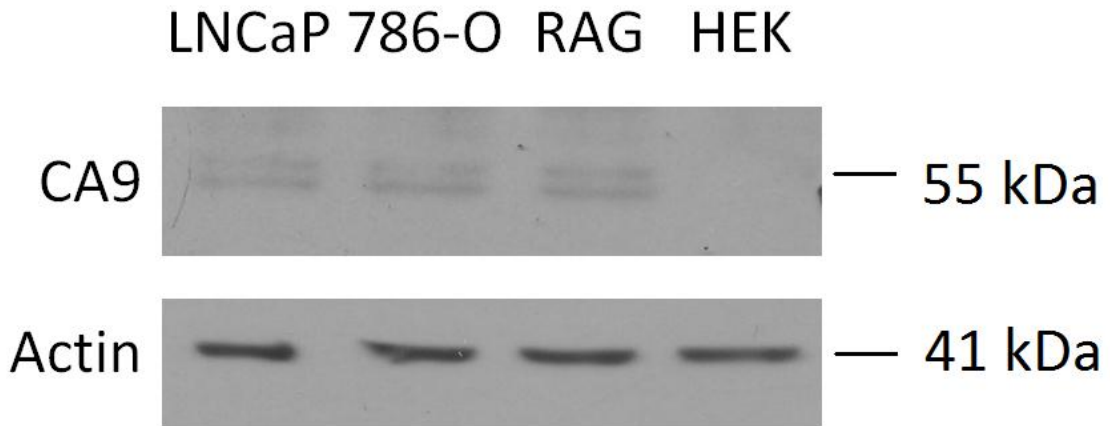


Fig. 4. Western blot analysis (SDS-PAGE run under reducing conditions) for carbonic anhydrase 9 in LNCaP, 786-O, RAG and HEK protein lysates. Calculated molecular weight is shown for CA9. Actin is shown as a loading control.

3.2 Knockdown of CA9 expression by shRNA in 786-O cells

As we hypothesize that CA9 confers radiation resistance in RCC, should RCC cells stop expressing the enzyme, their radiation tolerance should be reduced. To create a subcloned cell line with reduced expression, 786-O cells were transfected with shRNA targeting CA9 for knockdown (shCA9). Protein lysate samples were taken from 16 stable subclones and analyzed by Western blot analysis. The subclone with the highest knockdown of CA9 was selected (Fig. 5) for future experiments, registering only 8% (92% knock down) of the levels present in the accompanying scrambled shRNA control (shScr).

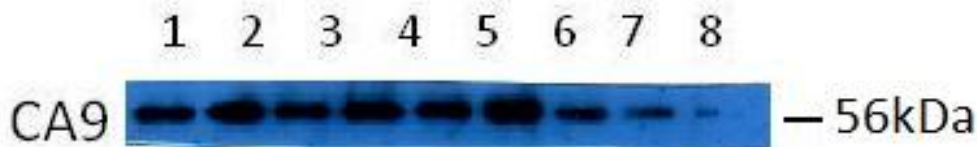


Fig. 5. Western blot analysis (SDS-PAGE run under reducing conditions) for carbonic anhydrase 9 in eight 786-O subclones transfected with shCA9. Number 8 was selected for future experiments. Calculated molecular weight is shown for CA9. See appendix C for shRNA sequence.

3.3 AEBS and shRNA can inhibit CA9 activity *in vitro*

AEBS is a known inhibitor of CA9's enzymatic reaction [75]. Therefore, to demonstrate its effectiveness in further *in vitro* experiments, a pH-indicator test was designed to measure the activity of the enzyme (Fig. 6a). In comparison to control untreated cells, incubation with either 33 μ M or 33 nM AEBS (99.9 and 50% inhibition of CA9 respectively [75]) caused significantly less absorbance change ($P < 0.001$). AEBS at 33 μ M produced 70% of untreated absorbance change while 33 nM produced only 36%. Wells with no cells present experienced a background absorbance change of only 11% compared to control cells, regardless of the presence or absence of AEBS.

AEBS was capable of a significant disruption of 786-O cells' ability to acidify the extracellular saline solution, supporting the idea that the compound is effective at inhibiting CA9 at *in vitro*. While the assay is not very specific with many contributing variables to acidification—such as anaerobic respiration and the metabolic creation of lactic acid—CA9's contribution seemed quite significant, which is unsurprising given it is one of the fastest enzymes known. The acidity change observed was not likely due to

the mere addition of the drug to the saline media, as wells without cells acidified at the same rate regardless of AEBS added. These wells did acidify slightly however, likely because CO₂ dissolution occurs without a catalyst, albeit slowly [44]. Using the assay solely with various concentrations of AEBS is insufficient to rule out non-specific inhibition of other carbonic anhydrases however. While AEBS has a very favourable K_i for CA9 (33 nM), the equilibrium has been shown more favourable still with CA12 as previously mentioned [75]—another transmembrane carbonic anhydrase. Furthermore, there may be other off-target effects of AEBS on 786-O cells that might slow acidification of media.

As further proof of concept for the CA9 activity assay and to exclude off-target effects by AEBS as the reason for the slowed acidification, shCA9 786-O cells were also used in the assay (Fig. 6b). The shCA9 cells had significantly decreased capacity ($P < 0.001$) to acidify media and experienced only 51% of expected absorbance change when compared to shScr cells. When experiments with AEBS and shCA9 are compared, the rate of acidification of the shCA9 cells fell close to the parental cells treated with 33 μM AEBS. ShScr cells were not significantly different from parental 786-O cells with respect to acidification.

These results demonstrate that AEBS's slowing of acidification was likely due to inhibition of CA9 as opposed to off-target interaction as the effect was duplicated when CA9 itself was knocked down by shRNA. The shScr 786-O cells were not significantly different than the untransfected cells, making the drug and knockdown experiments comparable and unlikely the knockdown's transfection itself had any effect on metabolic production of acid, aside from that of removing CA9.

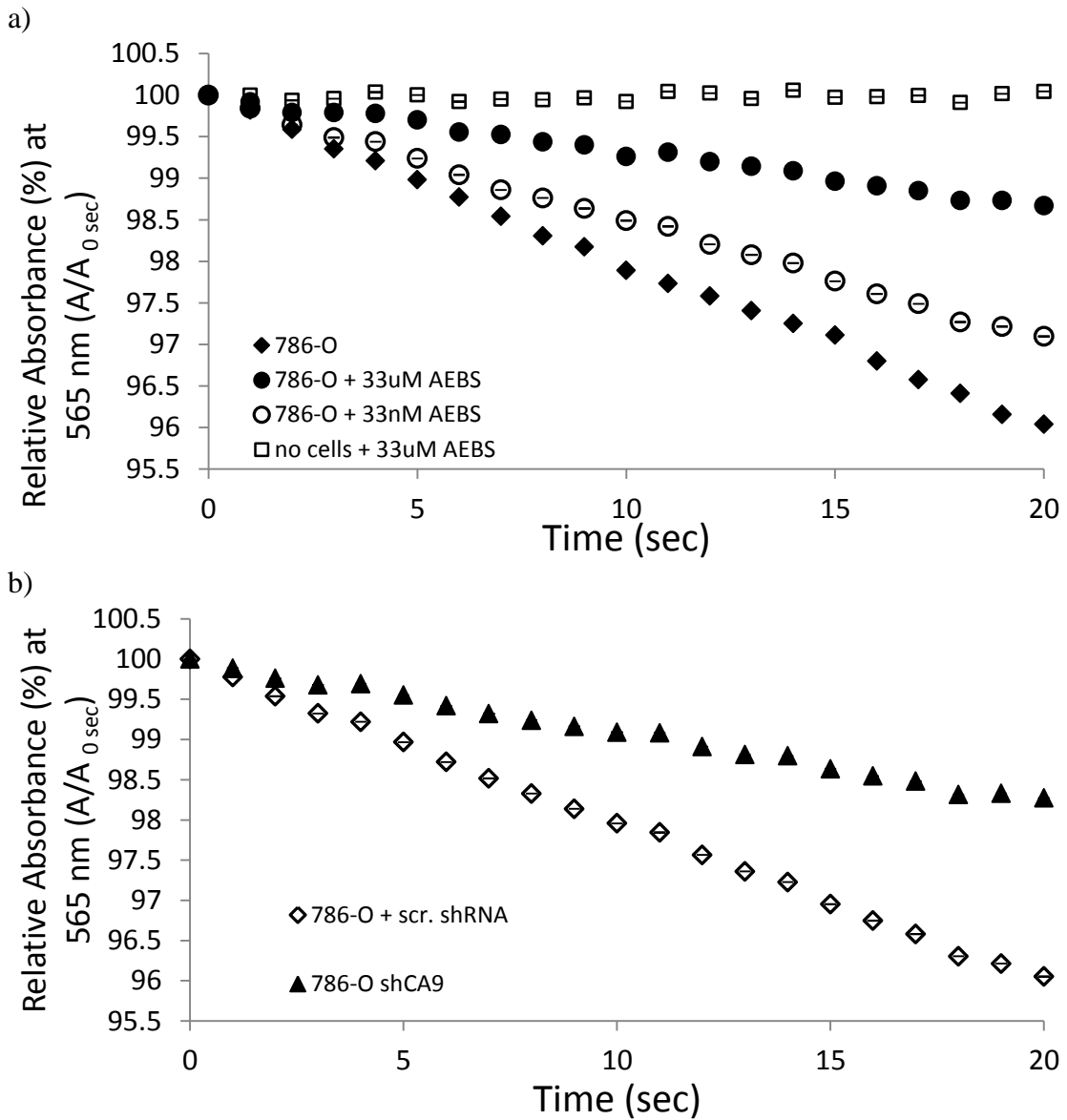
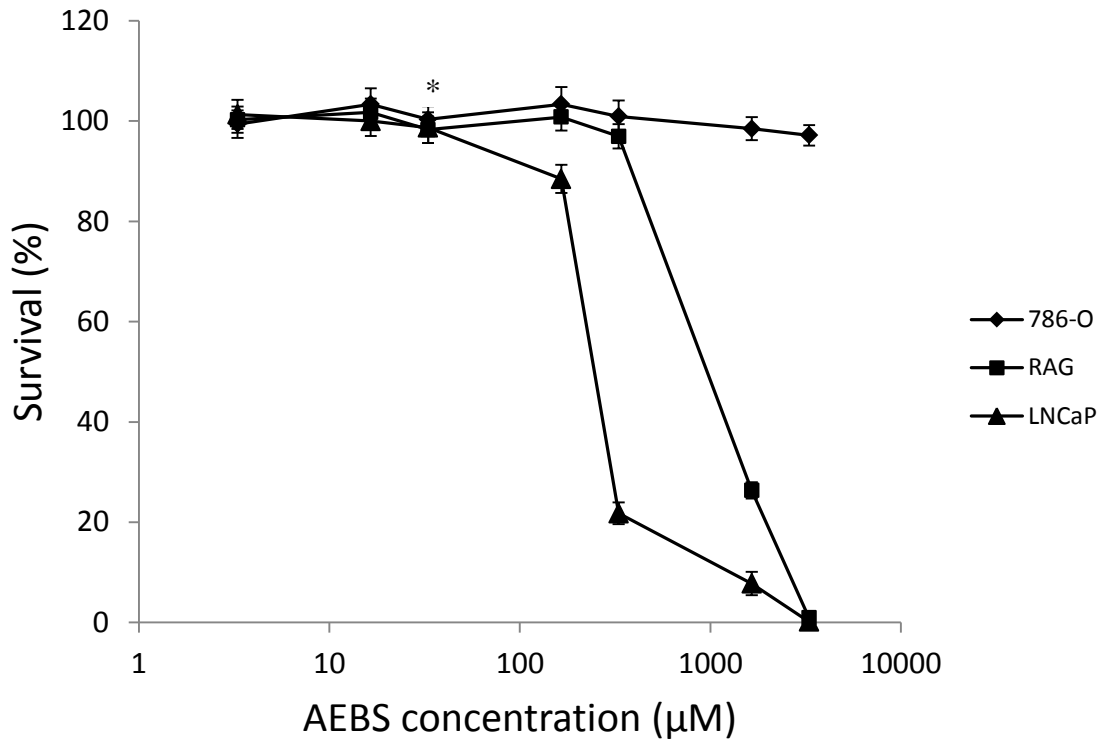


Fig. 6. Acidification of medium of 786-O cells a) in the presence or absence of AEBS b) expressing shCA9 or shScr as determined by the decrease in absorbance of phenol red over time. Decrease in absorbance is expressed as relative absorbance at 565 nm at a given time point (in sec) over the absorbance at time = zero. Background absorbance change is subtracted at each time interval. Error bars are \pm standard error of the mean for six experiments of one replicate.

3.4 AEBS is not toxic to 786-O cells *in vitro*

Another sulfonamide and inhibitor of CA9, acetazolamide, has been shown to induce apoptosis in HeLa and 786-O cells at 10 μ M and above [77]. A small percentage of people treated with sulfonamides experience severe allergic reactions while others remain symptomless [76] and there is very little published information on AEBS. To exclude toxicity as a confounding variable for future survival experiments, clonogenic survival assays were performed with 786-O, RAG and LNCaP cells to test the toxicity of AEBS (Fig. 7). Concentrations tested ranged from 0 to 3.3 mM. The 786-O cell line showed the most tolerance, with no significant reduction in surviving colonies at any of the drug concentrations tested. The RAG cell line had a calculated IC₅₀ of 1.36 mM, while the LNCaP cell line had an IC₅₀ of 413 μ M.

AEBS showed no significant toxicity or impairment of growth at 33 μ M. This demonstrates that inhibition of CA9 is not sufficient to cause a change in survival detectable by the clonogenic assay for these cell lines. It should be noted that the tolerance for the drug varies a great deal from only five times this concentration in some cell lines—namely LNCaP, to over 100 times in others—786-O cell line.



*33 µM is the concentration of AEBS required for 99.9% inhibition of carbonic anhydrase 9

Fig. 7. Toxicity of AEBS to 786-O cells, RAG cells and LNCaP cells as determined by clonogenic survival. Survival is expressed as a percent—at each given concentration of AEBS (in µM)—of survival at concentration = zero. Error bars are \pm standard error of the mean of six experiments of one replicate.

3.5 786-O and RAG cells are resistant to radiation *in vitro*

RCC tumours are considered radiation resistant, but it is unknown if this is merely a function of local tumour environment. Thus 786-O and RAG cells were irradiated with up to eight Gy and assessed in a clonogenic, *in vitro* survival experiment (Fig. 8). For comparison, the LNCaP (prostate adenocarcinoma) and LN-18 (glioblastoma) were included. The 786-O cell line displayed significantly more ($P < 0.001$) survival than the

others at a dose 2 Gy and above. Murine RAG cells displayed a comparable resistance to that of LN-18 cells. LNCaP cells displayed significantly less survival than other types ($P < 0.001$) at all doses. IC_{50} for 786-O, RAG, LN-18 and LNCaP was 3.52 Gy, 2.29 Gy, 1.94 Gy and 1.01 Gy respectively.

Glioblastomas such as LN-18 are considered amongst the most resistant types of cancer when it comes to radiation insults. Given the RAG cells had comparable resistance to the glioblastoma and the 786-O cells displayed an even greater tolerance for radiation, it seems that these two RCC cell lines are relatively resistant as well. It is important to note that the LNCaP line itself is considered to be relatively resistant to radiation [92], and that the RCC lines display even higher resistance still. This resistance is independent of a local tumour environment. The cells were seeded sparsely, meaning they were not under physical constraint. The media used had a significant pH buffering capacity centered around physiological conditions, meaning the low pH associated with tumour interiors was not a factor. Despite this, the cell lines displayed a significant tolerance to radiation insult, excluding local tumour environment as the sole reason for RCC's perceived resistance. Alternatively, it seems likely that a change in genetic or proteomic factors such as CA9 may be contributing to this phenomenon.

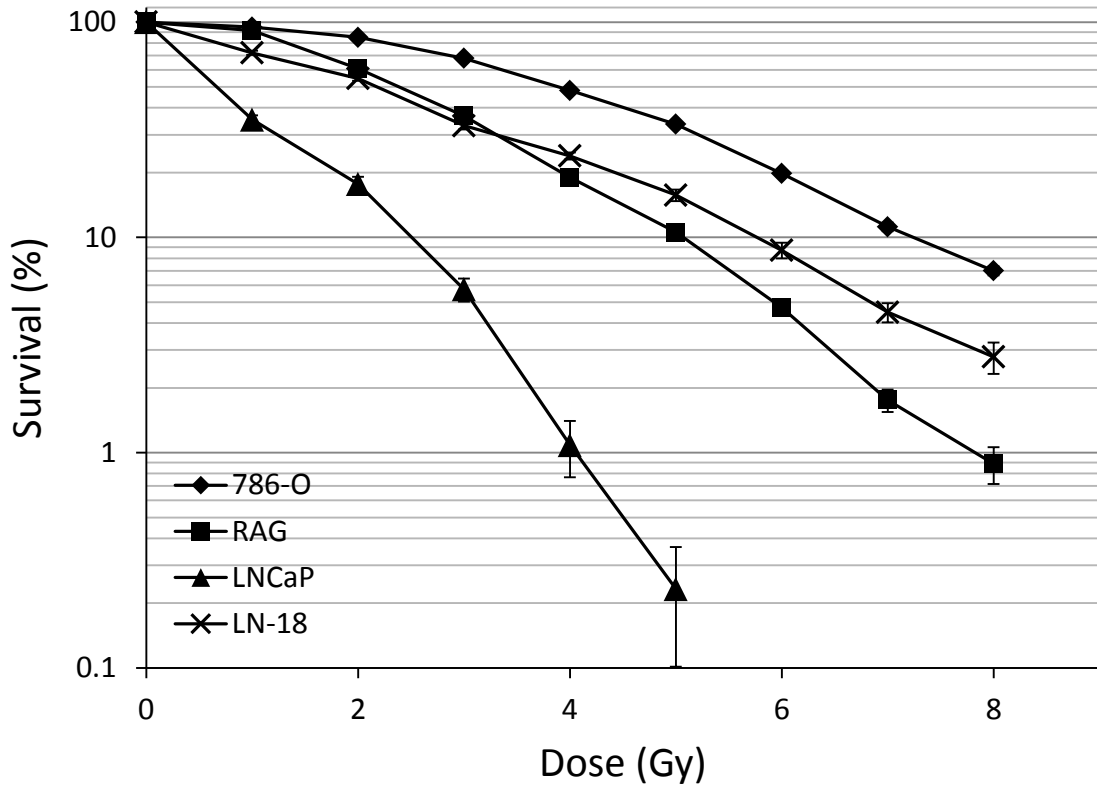


Fig. 8. Radiation resistance of 786-O cells, RAG cells, LNCaP cells and LN-18 cells as determined by clonogenic survival. Survival is expressed as a percentage—at each dose of six MV X-rays (in Gy)—of survival at dose = zero. Error bars are \pm standard error of the mean of 12 experiments of one replicate.

3.6 AEBS lowers radiation tolerance in 786-O and RAG cells, but not in LNCaP cells

To test the hypothesis that inhibiting CA9 promotes radiation sensitization, 786-O, RAG and LNCaP cells were irradiated with up to eight Gy of radiation in the presence or absence of AEBS (Fig. 9). The percent survival of 786-O cells was reduced significantly at doses of one through eight Gy ($P < 0.001$) when AEBS was present. The RAG cell line showed a similar, but less pronounced reduction in survival at these doses

of radiation in the presence of AEBS ($P \leq 0.018$). LNCaP cells displayed no significant reduction in survival at any dose of radiation in the presence of AEBS.

The significant reduction in the radiation tolerance of the renal carcinoma cell lines (786-O and RAG) when CA9 was inhibited by AEBS points to CA9 as a possible conveyor of such tolerance. However, no significant reduction of survival was seen in the prostate adenocarcinoma LNCaP cell line. As previously mentioned, the LNCaP cell line does reportedly not express CA9 [90], yet we detected it by our Western blot analysis in similar amount as observed in 786-O and RAG cells. As it has been shown that reporter genes regulated by the HRE (Hypoxia Responsive Element) may be 150–250 fold induced when LNCaP cells are seeded densely [93], it is possible that CA9 is only expressed in LNCaP cells under these conditions. As cells are seeded very sparsely in the clonogenic survival assays, one would expect little CA9 to be expressed. Thus the cell line should display no sensitivity to CA9 inhibitors if none is expressed in the clonogenic assay, despite having the lowest tolerance for higher concentrations of the drug (Fig. 7). It is also possible that the ability of the enzyme to affect radiation tolerance may be specific to certain types of tissues or cancers, depending on their genomic and/or proteomic state. Nonetheless, it is encouraging that a small molecule drug with potential for use in patients can lower resistance in RCC. This is especially true if cells not expressing CA9 are unaffected by the drug. As most normal tissues do not express CA9 [59], AEBS may provide an effective way of targeting patients' tumours specifically for radiosensitization.

Cells whose radiation survival curves are linear and proportional to dose such as LNCaP, are generally thought to be repair-deficient and/or prone to apoptosis upon

receiving significant DNA damage [104]. Conversely, cells that avoid or are deficient in apoptotic pathways and/or tend towards DNA repair have large “shoulder” regions at lower doses [104]. In this experiment, the cells with the widest “shoulders” in their survival curves appeared to be most antagonized by the inhibition of CA9. This hints at CA9 playing a role in either promotion of DNA repair, suppression of apoptosis or both.

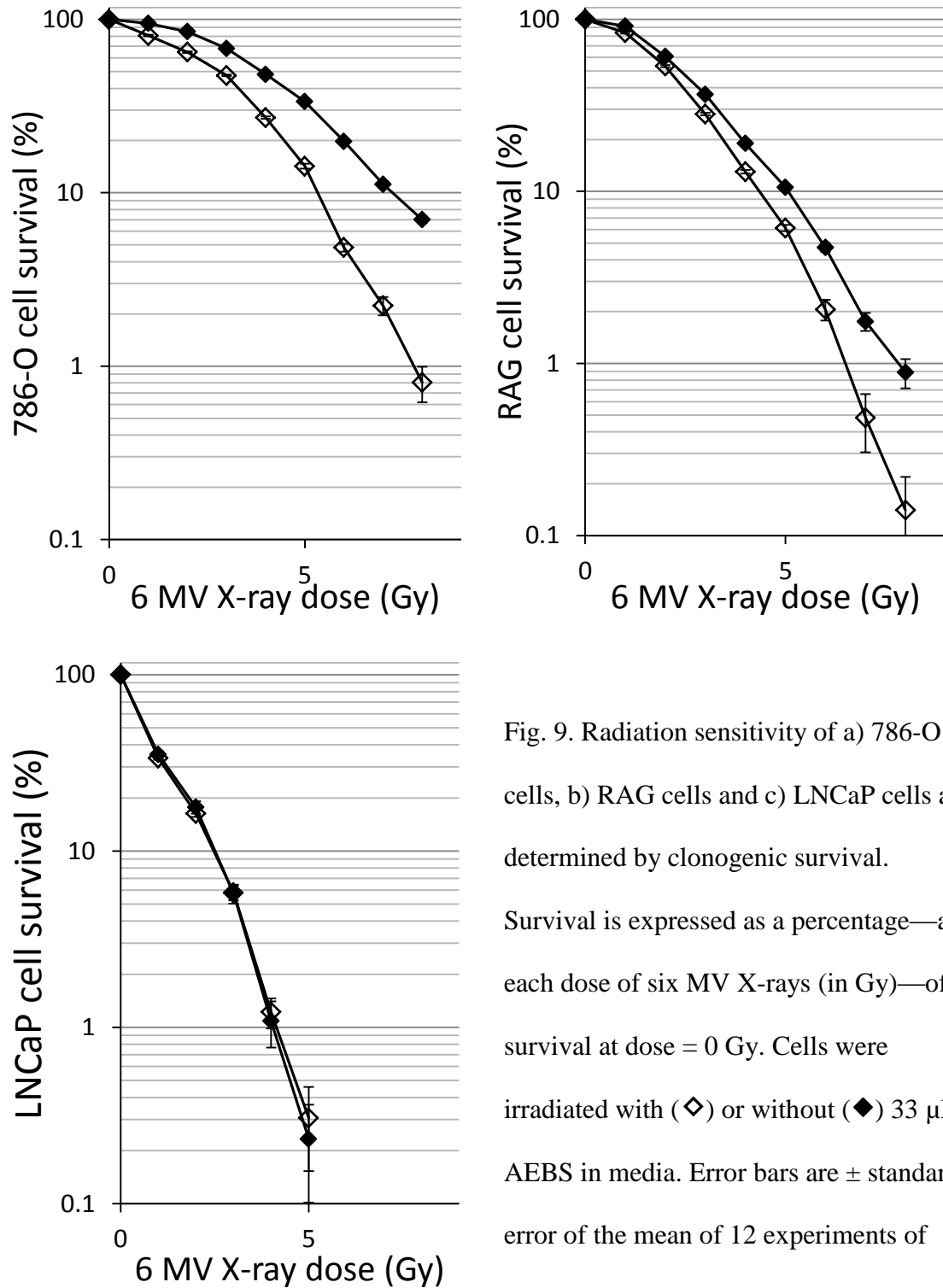


Fig. 9. Radiation sensitivity of a) 786-O cells, b) RAG cells and c) LNCaP cells as determined by clonogenic survival. Survival is expressed as a percentage—at each dose of six MV X-rays (in Gy)—of survival at dose = 0 Gy. Cells were irradiated with (◇) or without (◆) 33 μM AEBS in media. Error bars are ± standard error of the mean of 12 experiments of one replicate.

3.7 786-O cells expressing shCA9 have decreased radiation tolerance

To support the hypothesis that CA9 confers radiation tolerance in RCC, 786-O cells stably transfected with shCA9 were irradiated. In comparison to the shScr control cells, the percent survival of the knockdown subclone was significantly lower ($P < 0.001$) at a dose of one Gy and above (Fig. 10).

Knocking down CA9 as opposed to merely inhibiting the enzyme reproduced the same phenomenon of decreased radiation tolerance in 786-O cells. This supports the hypothesis that the enzyme is involved in conferring resistance to radiation, but also that the decrease in survival caused by AEBS is due to its targeting of CA9 and not toxicity.

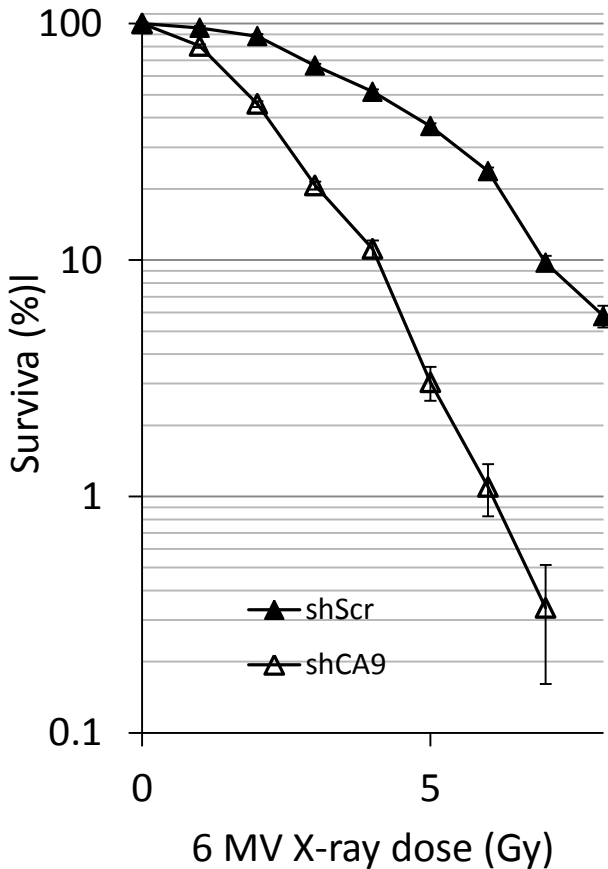


Fig. 10. Radiation sensitivity of transfected 786-O cells shScr (▲) and shCA9 (△) as determined by clonogenic survival. Survival is expressed as a percentage—at each dose of six MV X-rays (in Gy)—of survival at dose = zero. Error bars are \pm standard error of the mean of 12 experiments of one replicate.

3.8 Reduced CA9 expression sensitizes 786-O cells to radiation more so than inhibition by AEBS

When the survival data for 786-O cells with CA9 knocked down 92% and inhibited with 33 μ M are compared (Fig. 11), the knockdown cell line displays significantly less radiation tolerance than the cell line which is merely inhibited at two Gy and higher ($P < 0.001$). The survival of the scrambled and untransfected subclone is not significantly different.

If the enzymatic activity (dissolution of CO₂) of CA9 were the mechanism by which radiation tolerance is promoted in 786-O cells, one would expect a 92% knockdown of the enzyme to be roughly 92% as effective as 99.9% inhibition of the active site. It is therefore counter-intuitive to find that the knockdown was significantly more sensitive, which suggests that while the catalytic activity of CA9 is somewhat important for conferring radiation resistance, other aspects of the enzyme—CA9's intracellular tail or extracellular proteoglycan domain perhaps—may contribute to this phenomenon as well. This supports the idea that the phosphorylation of CA9 at tyrosine residues may suppress apoptosis. Clinically, this presents an opportunity for drugs targeting CA9 by interference with its expression, a strategy that may well be more effective than targeting the enzyme directly. Moreover the acidification of the extracellular environment that is driven by the enzyme is unlikely to be the cause of this resistance because the media the cells grow in is highly pH-buffered. It has been suggested that inhibition of CA9 may disrupt intracellular pH however, possibly causing apoptosis [77]. The shScr and parental 786-O subclones display no significant survival

difference—the parental cells having received mock drug additions while the shScr line did not.

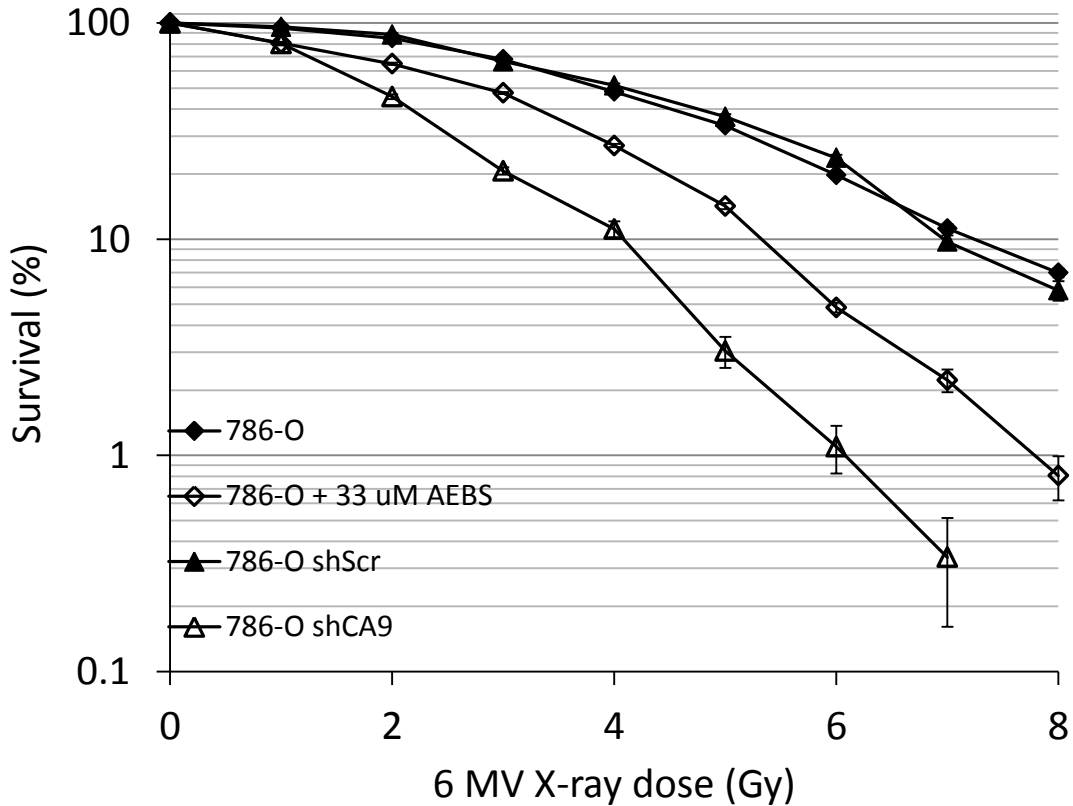


Fig. 11. Comparison of radiation sensitization of 786-O cells by AEBS or shCA9 as determined by clonogenic survival. Survival is expressed as a percentage—at each dose of six MV X-rays (in Gy)—of survival at dose = zero. Error bars are \pm standard error of the mean.

3.9 AEBS or shCA9 radiation tolerance loss is more pronounced if the radiation dose is fractionated

To investigate if a fractionated regimen of radiation delivery could increase the survival difference between CA9-inhibited and non-inhibited RCC cells, 786-O cells with and without the addition of AEBS to the medium were subjected to three treatments of

two Gy spread over three consecutive days (Fig. 12). 786-O cells expressing shScr or shCA9 received the same treatment. Cells receiving AEBS or expressing shCA9 had significantly reduced survival ($P < 0.001$) after receiving fractionated radiation treatment, similar to single dose trials, also displayed in Fig. 12 for reference.

As previously shown, either the addition of 33 μM AEBS to 786-O cells or transfection with shCA9 prior to irradiation lowers survival significantly. For instance, at two Gy, the addition of AEBS allows only 76.2% of cells that would have survived to do so (see Fig. 9a). If such a treatment were to be repeated, ideally this difference should be multiplicative and become larger with every fraction delivered. The results of this fractionation experiment support this idea. When receiving AEBS, only 51.5% of expected 786-O cells survived (Fig. 12). As the convention for radiation therapy involves fractionation, the increased effectiveness of the drug under these conditions increases AEBS' appeal for use in the clinic. Similarly, with one fraction of two Gy, 51% of cells expressing shCA9 survive that were expected to without. After three fractions, only 35.7% of shCA9 cells survive that are expected from shScr controls. This reduction in survival again underscores the importance of CA9 in the radiation resistance of 786-O cells and is consistent with the conjecture that the enzyme may be related to either the promotion of DNA repair after consecutive radiation insults or to the suppressing of apoptotic signals as damage is incurred by the cell between such fractionations.

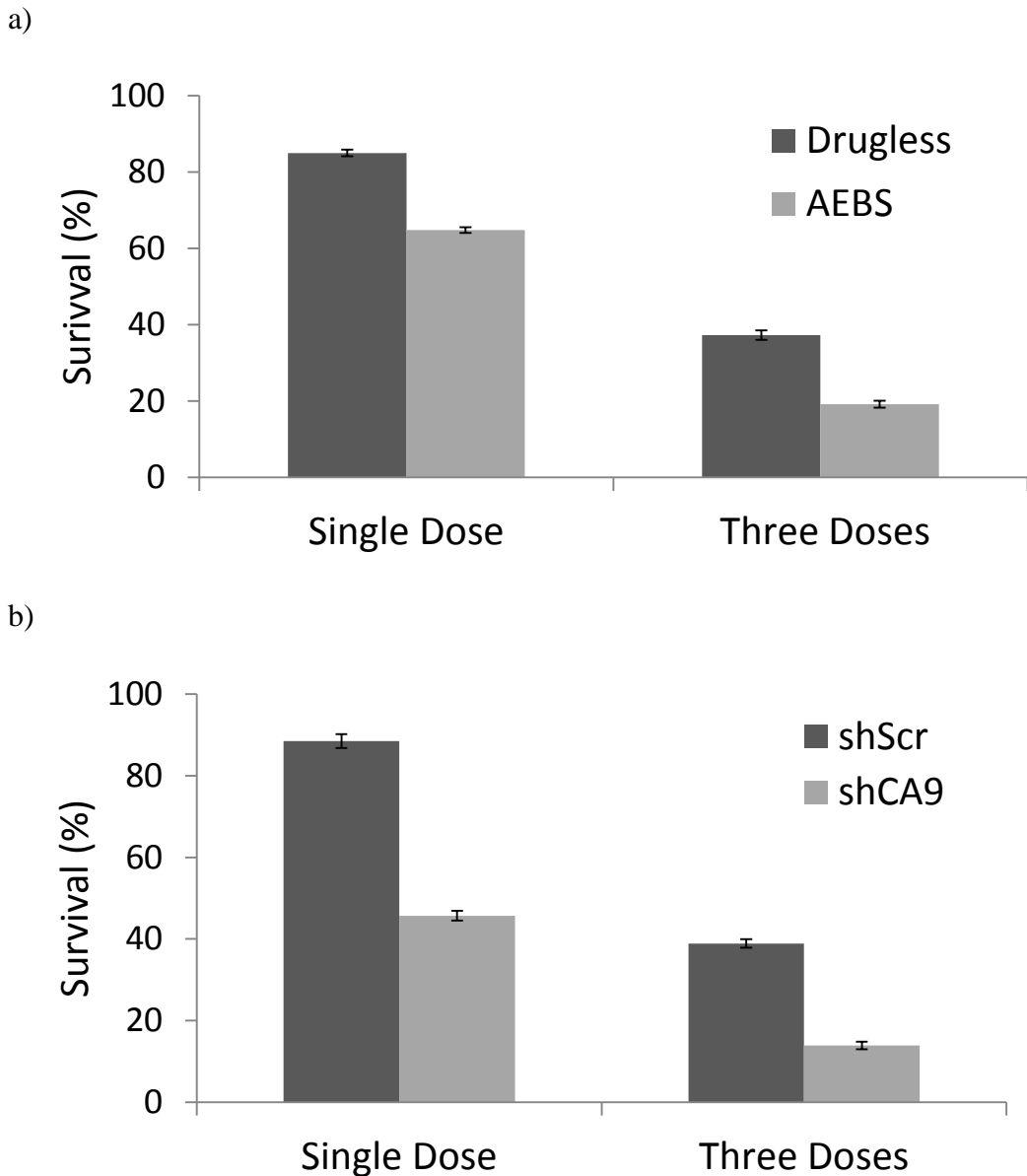


Fig. 12. Radiation sensitivity of 786-O cells receiving a fractionated radiation regimen a) in the presence or absence of AEBS and b) expressing shRNA against CA9 as determined by clonogenic survival compared with single-dose experiments. Survival is expressed as a percentage—under each condition—of survival with no treatment administered. Fractions consisted of two Gy doses of six MV X-rays delivered once or once every 24 hr for three days. Error bars are \pm standard error of the mean.

3.10 ShCA9-expressing 786-O tumours have decreased tolerance for radiation *in vivo*

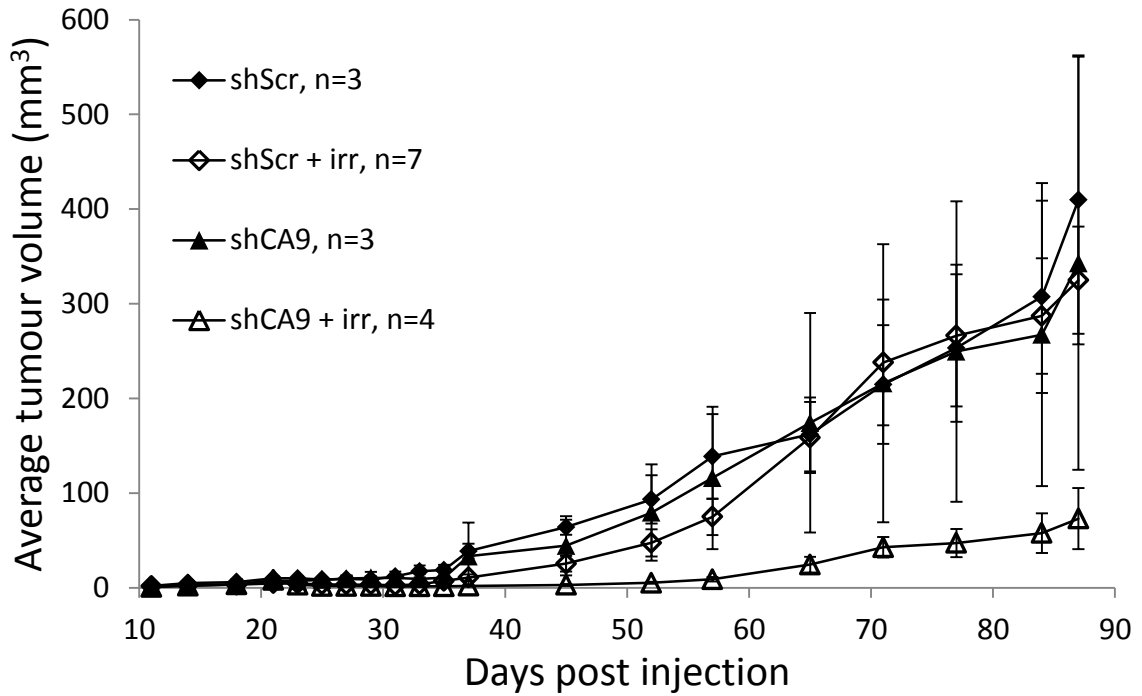
In order to assess whether or not the targeting of CA9 might be applied practically for eventual clinical use, a murine experiment was carried out to simulate *in vivo* radiation therapy conditions. Mice were injected with one million 786-O cells expressing shScr or shCA9. The tumours were allowed to grow and irradiated or mock irradiated three weeks later with tumour volume being measured 1-3 times weekly (Fig. 14a). Tumour take rate was 30% in non-irradiated groups, 40% in the shCA9 irradiated group and 70% in the shScr irradiated group. There was no significant difference in tumour volume between shScr (irradiated or mock) and mock-irradiated shCA9 tumours. Beyond 52 days post-injection however, irradiated shCA9 tumours were significantly smaller ($P < 0.05$) than the irradiated shScr tumours. The final weights of the tumours (Fig. 14b) displayed the same pattern. Statistically significant differences between all groups were not found except between irradiated groups shScr and shCA9 ($P < 0.05$). Hence by both volume and by mass, shCA9 786-O cells were significantly smaller ($P < 0.05$) than the shScr control when irradiated.

CA9 levels in tumour homogenates were confirmed to be significantly ($P < 0.05$) suppressed by Western blot (Fig. 15) with densitometric analysis (Fig. 16) at 2.8% in the shCA9 irradiated group and 21.3% in the shCA9 mock-irradiated group when compared to shScr tumours in the mock-irradiated group. A typical H&E staining of tumour tissue in each group is shown in Fig. 17.

The lack of significant difference between irradiated and mock-irradiated shScr tumours is a testament to the radiation resistance of RCC; the volumes of the irradiated

shScr tumours reached parity with mock-irradiated tumours relatively quickly. The negligible difference between mock-irradiated shScr and shCA9 tumours shows that CA9 may not play a large role in sheer growth rate, despite being involved in mitigating the negative effects of rapid growth such as hypoxia. The significantly smaller irradiated shCA9 tumours however point to CA9 being critical to radiation resistance. This group which expressed far less CA9 seemed to suffer the most harm from radiation, only recovering to a quarter the size of their similarly irradiated non-knockdown counterparts. It would therefore seem that CA9 is important for RCC's radiation resistance *in vivo* as well as *in vitro*. Hypoxia, physical constraint, pH and other *in vivo* factors may still contribute the RCC's radiation resistance, but may not be as important as previously considered. Before hypoxia is dismissed completely however, it should be noted that tumours were fairly small (most under 20mm³) upon irradiation in this experiment, and not likely to be significantly hypoxic at that stage of growth. In summary, the concurrent targeting of CA9 with radiation therapy may well be useful for clinical use in so far as it seems to produce significant tumour control and/or killing power.

a)



b)

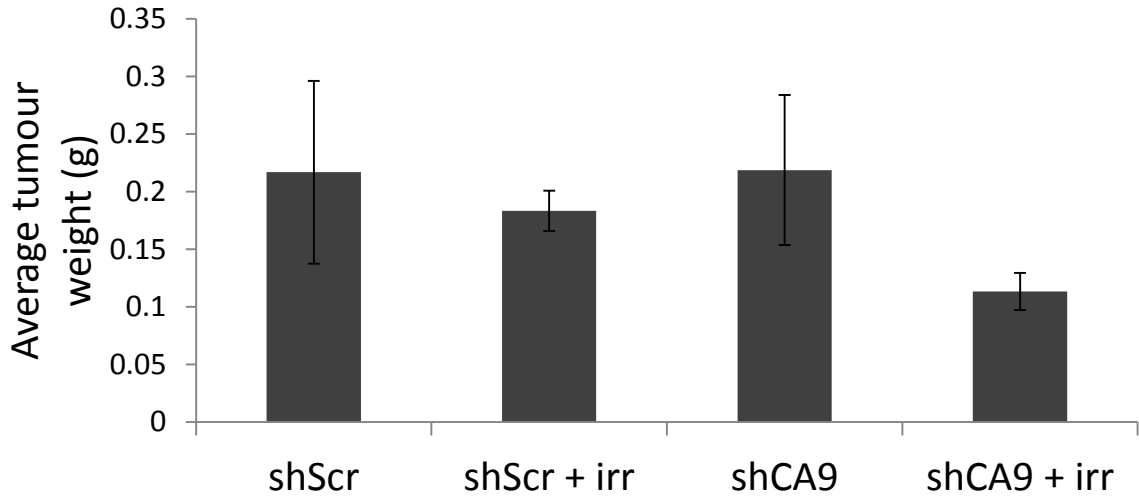


Fig. 13. Average tumour size by a) volume in mm³ and b) weight in grams of subcutaneous 786-O tumours expressing shScr or shCA9 in BALB/c NU/NU mice.

Tumours were irradiated (Irr) or mock-irradiated with six Gy on day 21. Error bars are \pm standard error of the mean of 3–7 tumours per group.

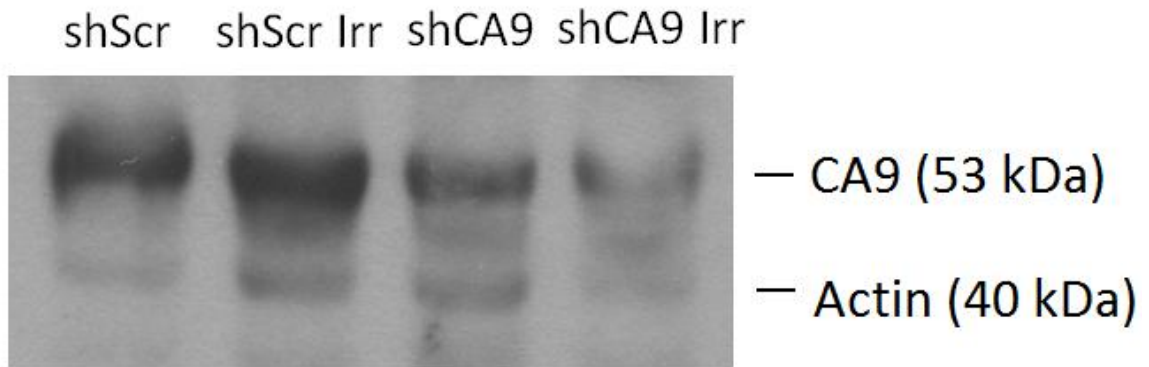


Fig. 14. Western blot analysis (SDS-PAGE run under reducing conditions) for carbonic anhydrase 9 in tumour homogenates. Calculated molecular weight is shown for CA9.

Actin is shown as a loading control.

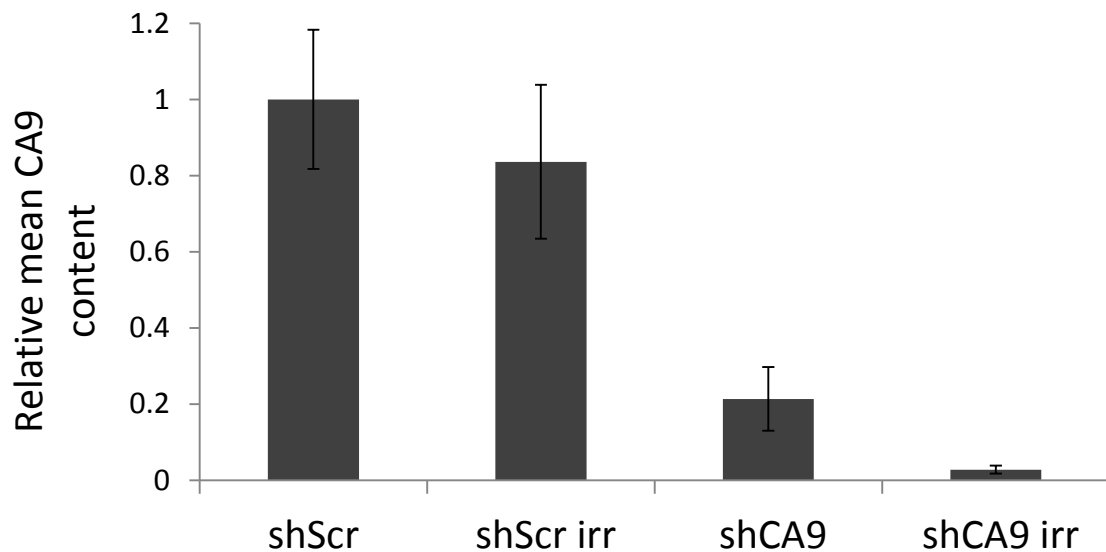
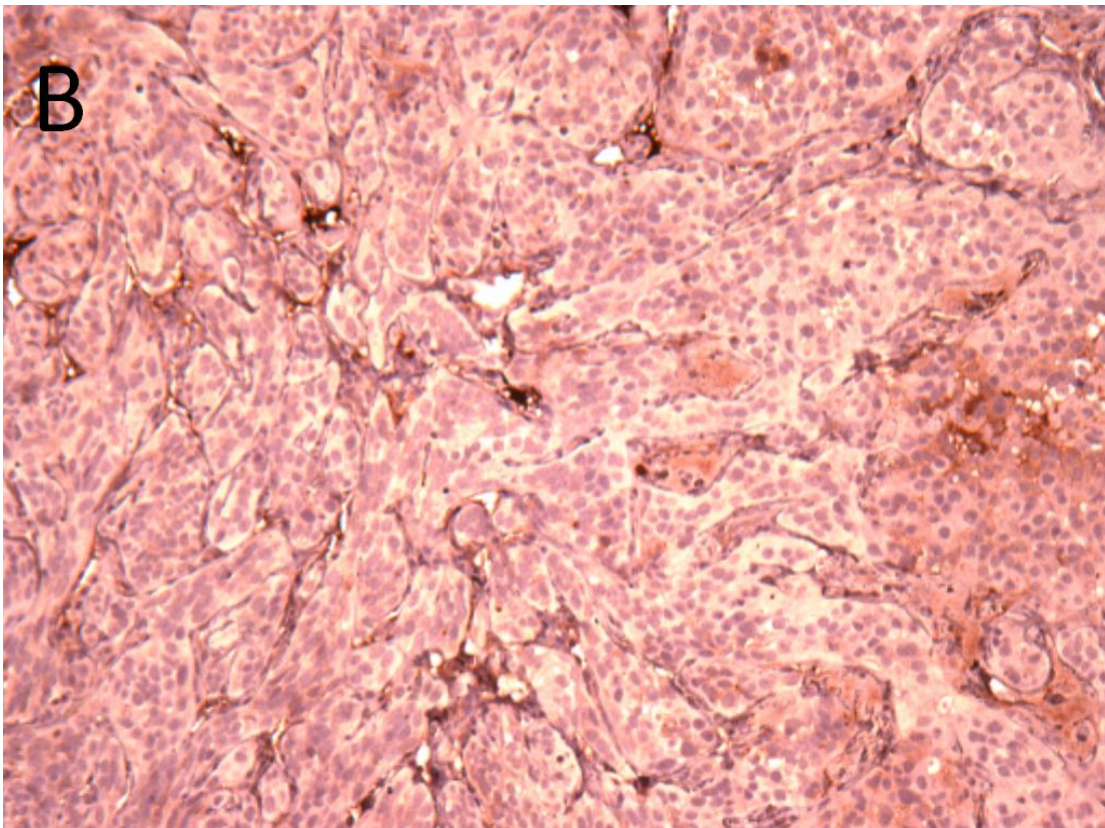
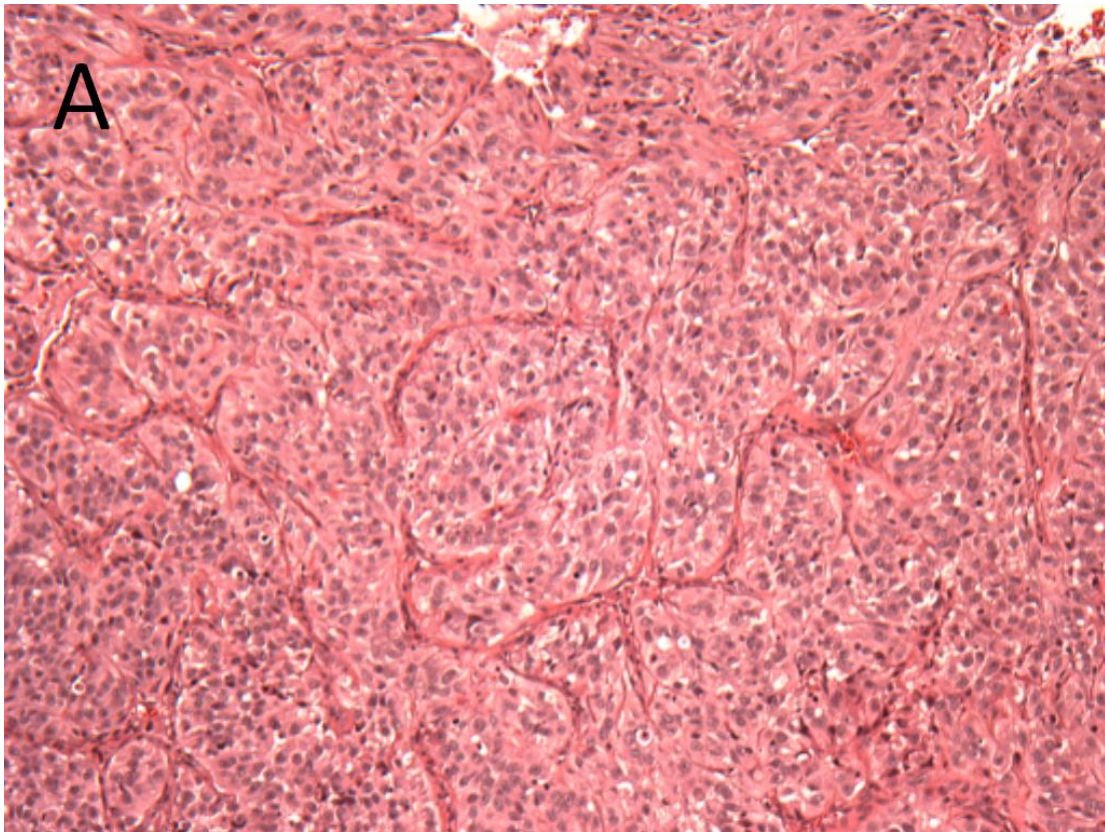


Fig. 15. Mean CA9 protein content in tumour xenograft homogenates as a ratio of the shScr tumour homogenate mean. Error bars are \pm standard error of the mean. CA9 protein content was divided by actin content.



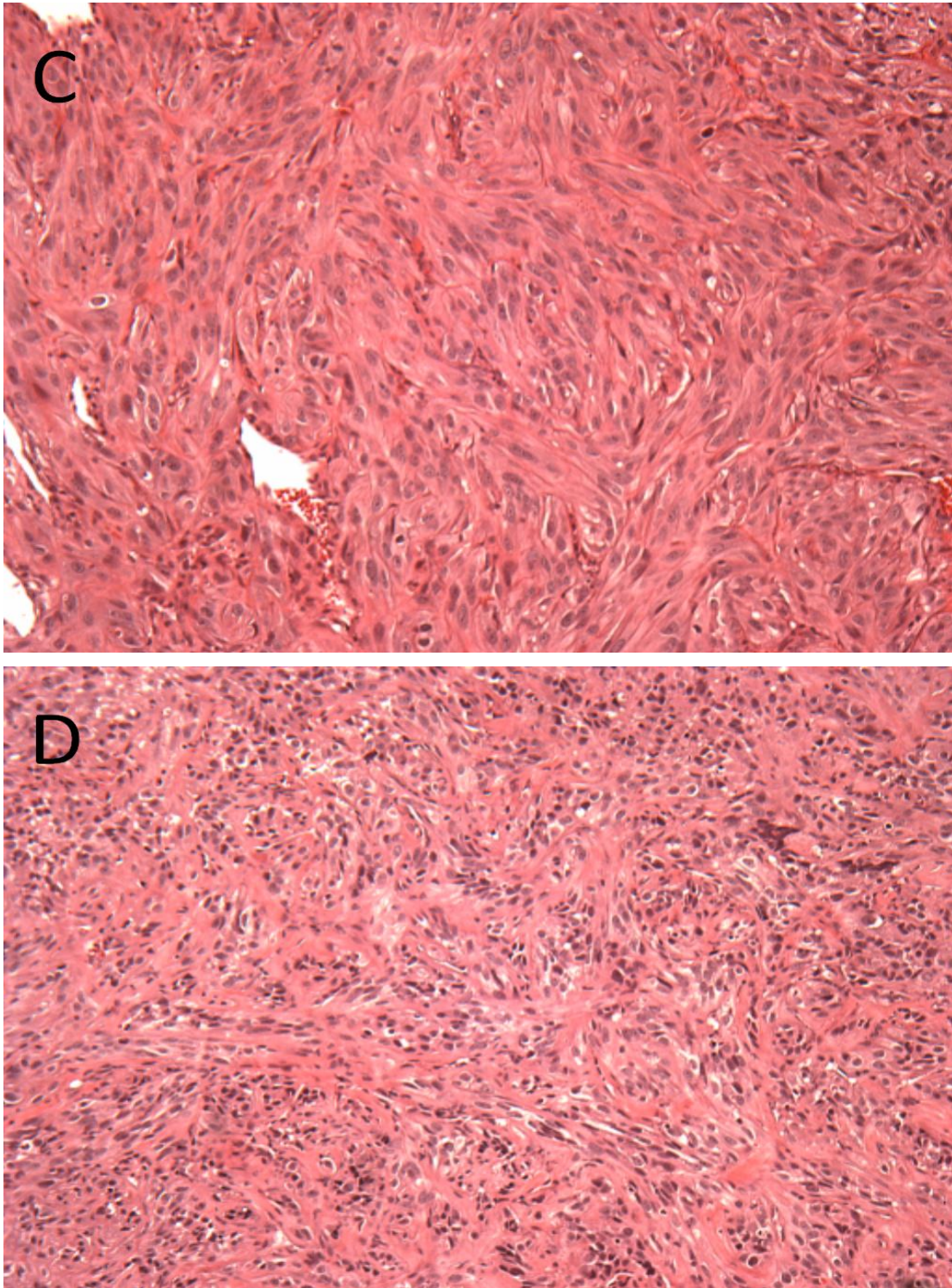


Fig. 16. Representative hemotoxylin and eosin stain of xenograft tumour tissue removed from mice in A) shScr/mock-irradiated B) shScr/irradiated C) shCA9/mock-irradiated and D) shCA9/irradiated groups.

4.0 Conclusion

4.1 Summary

RCC tumours are considered resistant to radiation, largely eliminating treatment with radiation therapy as a viable option for patients. To demonstrate this radiation resistance, RCC cell lines 786-O and RAG were compared alongside the more notoriously resistant cell lines LNCaP and LN-18 (prostate adenocarcinoma and glioblastoma) in clonogenic survival experiments. After being subjected to up to eight Gy of X-rays, the 786-O cell line displayed greater survival than the LN-18, while both RAG and 786-O RCC cell lines demonstrated greater radiation resistance than the LNCaP. As glioblastomas especially are amongst the most resistant cell lines known [94], the comparable resistance of the RCC lines confirms that they too may be counted as such. Moreover, the *in vitro* nature of the experiment demonstrates that local tumour environment factors such as acidity, hypoxia or physical constraint may not as significant a role in the radiation resistance of RCC as previously thought.

To demonstrate carbonic anhydrase 9's role as contributor to radiation resistance, the enzyme was targeted in RCC cell lines 786-O and RAG by the small molecule inhibitor AEBS while cells were concurrently irradiated with up to eight Gy of X-rays. The addition of AEBS significantly lowered the survival of these cell lines, suggesting that the drug can radio-sensitize RCC by inhibition of CA9. Drug toxicity was excluded as a confounding factor as the presence of drug itself did not cause a reduction in survival at relevant concentrations for cell lines tested. Sensitization was not seen in the prostate LNCaP line however, despite the presence of CA9 detected in cell lysate. This may be due to the hyper-inducible nature of HIF-1 under hypoxic conditions. Lysates taken from

confluent dishes may have expressed large amounts of CA9, while the enzyme was not present when the cells were seeded sparsely in the clonogenic experiment. It is also noteworthy that LNCaP cells have not been previously reported to express CA9; it has possibly gone undetected due to this extreme variance in expression.

A similar increase in RCC's sensitivity is seen when the enzyme's expression is suppressed in 786-O cells by RNA silencing, again suggesting that CA9 is a contributor to radiation-resistance. Moreover, it seems that the silencing of the enzyme's expression is more effective at sensitizing cells to radiation than inhibition of the active site. This points to other functions of the enzyme being involved as well, such as the binding of phosphorylated CA9 to PI3K and the activation of AKT. These results are therefore consistent with the idea that CA9 is acting as an apoptotic suppressor. Furthermore the shape of the survival curves, namely the elimination or reduction of the shoulder region, suggests cells are more likely to undergo apoptosis and forego attempts at repair when inhibitor or lower amounts of CA9 are present.

The *in vitro* conditions of these experiments are not necessarily a good model for the growth of three-dimensional RCC tumours, lacking factors such as physical constraint, hypoxia and pH change. Yet when 786-O cells with or without CA9 knocked down were allowed to form tumours in the murine experiment presented here, tumours with CA9 knocked down suffered most from irradiation. The tumours expressing less CA9 had a significantly smaller mass and measured volume than the control when tumours received radiation. Although sample size was small, this suggests that the contribution of CA9 to radiation resistance in RCC holds true *in vivo* as well and *in vitro*. Furthermore, this increases the feasibility of targeting the enzyme in patients receiving

radiation therapy for RCC. It also demonstrates that tumour environment may not be that important a factor for radiation resistance.

The serious problem of radiation resistance in RCC has thus far prevented the benefits of radiation therapy from being accessed by patients. Here we present a possible cause of this problem as well as a possible solution. Carbonic anhydrase 9 represents an appealing target for inhibitors or antagonists of its expression in RCC when supplemented with radiation therapy. Either inhibiting or reducing expression seems to reduce the tolerance of the disease to radiation *in vitro* with the latter effective *in vivo* as well. Moreover, a fractionated delivery of radiation seems to amplify this effect when CA9 is silenced or inhibited. Thus a drug treatment targeting CA9 will likely work well in a typical radiation treatment regimen.

The final goal of the research presented here is to allow patients to benefit from having an additional option for treatment of their RCC. It is hoped that inhibition of CA9 along with radiation therapy may in time become a substitute for partial and radical nephrectomies. This would allow patients to retain greater kidney functioning post-treatment and forego the risk of infection and surgical complications. Altogether, radiation therapy for RCC may be an increasingly viable option if CA9 can be successfully inhibited concurrently.

4.2 Future work

In vitro experiments are useful not only as models, but in their own light as well. The resistance of RCC to radiation has been traditionally believed a symptom of hypoxia or an acidic local environment in the tumour. However, as the resistance of multiple RCC cell lines has now been demonstrated in normoxic and pH buffered conditions of media,

this hypothesis seems at best only partially true; changes in the expression profile of such cells may contribute to this phenomenon as well. While these factors likely do contribute to radiation tolerance in RCC, the degree to which they do remains unknown. It would be useful to know this for the purposes of *in vivo* use where hypoxia and pH are not controlled. The *in vivo* experiment presented here suggests these are negligible factors; however, the tumours treated were not in a typical location for RCC. Primary RCC tumours are not found under a millimetre of epidermis, but in the kidney itself. It is possible that the resistance of RCC depends as well on the depth of the tumour and dose deposition in humans; something not simulated here.

The eventual use of AEBS clinically would require more in-depth and long term evaluation *in vivo*. As previously mentioned, similar sulphonamides have been used as diuretics and in lieu of antibiotics with minimal side effects. We have assumed up to this point as AEBS is an inhibitor of CA9, that only cells expressing CA9 should be adversely affected by it. This is not necessarily true of course, as toxicity may arise from other interactions not found here. A murine, *in vivo* experiment using AEBS would be beneficial as it would provide the required dose to see an appreciable effect and provide useful toxicity information necessary before proceeding to human trials. Given the experiment here used a stable genetic knockdown, it is unknown whether the results can be duplicated *in vivo* with an inhibitor. It also may be that interference with CA9 is required just as much during tumour recovery after irradiation as during irradiation itself. Consistent administration of AEBS might be required post-irradiation; if targeting CA9 does work through suppression of apoptosis, then this could well be the case.

It may be worth investigating the finding of CA9 in LNCaP cells as they have previously been thought to not be expressed by this cell line. In fact, LNCaP cells have been used as a negative control for CA9 [90]. We have postulated that this may be due to the hyper-inducible nature of HIF-1 in this cell line, but nothing has yet been done to show that this is the case. It may also be that unique *de novo* mutations have led to CA9's expression in our cultures. It is also worth noting that the media used was not standard—it contained additional bicarbonate to increase pH buffering capacity and additional non-essential amino acids. Either of these may have led to a difference in reported expression of CA9.

AEBS, while fairly specific to CA9, is also an efficient inhibitor of CA12 as previously mentioned. As CA12 is also known to be associated with various types of cancer [105], and is also membrane-bound, it may represent a confounding variable for the effects of AEBS. Whether or not the cell lines studied here express CA12 should be determined. If it is expressed in these cell lines, it would be necessary to determine if it plays a significant role in the radio-sensitivity effects demonstrated here.

While we suspect CA9 increases radiation tolerance through the suppression of apoptosis, this has yet to be shown directly. Demonstrating how this phenomenon actually works would be useful as it may open up the possibility of reducing radiation tolerance by other means. If the apoptotic pathway through EGF signalling is indeed being suppressed, other targets may become available. Preventing the phosphorylation of CA9 by EGFR may produce the same result, or perhaps prevention of PI3K from interacting with CA9. Other unrelated pro-apoptotic drugs may work synergistically with

anti-CA9 therapies, etc. Overall, targeting CA9 to reduce radiation resistance in RCC is a new field with many unknowns and possibilities.

References

1. Siegel R, Naishadham D, Jemal A (2012) Cancer statistics, 2012. *CA Cancer J Clin* 62: 10-29.
2. http://www.engin.umich.edu/~cre/web_mod/viper/kidney_function.htm. Accessed 01/14/13
3. Navai N, Wood CG (2012) Environmental and modifiable risk factors in renal cell carcinoma. *Urol Oncol* 30: 220-224.
4. Pavlovich CP, Schmidt LS (2004) Searching for the hereditary causes of renal-cell carcinoma. *Nat Rev Cancer* 4: 381-393.
5. Sun M, Shariat SF, Cheng C, Ficarra V, Murai M, et al. (2011) Prognostic factors and predictive models in renal cell carcinoma: a contemporary review. *Eur Urol* 60: 644-661.
6. Lakmichi MA, Jarir R, Kabour J, Dahami Z, Said Moudouni M, et al. (2011) Sciatica leading to the discovery of a renal cell carcinoma. *Pan Afr Med J* 9: 18.
7. Patel C, Ahmed A, Ellsworth P (2012) Renal cell carcinoma: a reappraisal. *Urol Nurs* 32: 182-190; quiz 191.
8. Gibbons RP, Monte JE, Correa RJ, Jr., Mason JT (1976) Manifestations of renal cell carcinoma. *Urology* 8: 201-206.
9. Stec R, Grala B, Maczewski M, Bodnar L, Szczylik C (2009) Chromophobe renal cell cancer--review of the literature and potential methods of treating metastatic disease. *J Exp Clin Cancer Res* 28: 134.
10. Ross H, Martignoni G, Argani P (2012) Renal cell carcinoma with clear cell and papillary features. *Arch Pathol Lab Med* 136: 391-399.
11. Deng FM, Melamed J (2012) Histologic variants of renal cell carcinoma: does tumor type influence outcome? *Urol Clin North Am* 39: 119-132, v.
12. Phillips TL, Fu KK (1976) Quantification of combined radiation therapy and chemotherapy effects on critical normal tissues. *Cancer* 37: 1186-1200.
13. (1991) 1990 Recommendations of the International Commission on Radiological Protection. *Ann ICRP* 21: 1-201.
14. Escudier B, Bellmunt J, Negrier S, Bajetta E, Melichar B, et al. (2010) Phase III trial of bevacizumab plus interferon alfa-2a in patients with metastatic renal cell carcinoma (AVOREN): final analysis of overall survival. *J Clin Oncol* 28: 2144-2150.
15. Al-Marrawi MY, Rini B (2011) Pazopanib for the treatment of renal cancer. *Expert Opin Pharmacother* 12: 1171-1189.
16. Escudier B, Eisen T, Stadler WM, Szczylik C, Oudard S, et al. (2009) Sorafenib for treatment of renal cell carcinoma: Final efficacy and safety results of the phase III treatment approaches in renal cancer global evaluation trial. *J Clin Oncol* 27: 3312-3318.
17. Motzer RJ, Hutson TE, Tomczak P, Michaelson MD, Bukowski RM, et al. (2007) Sunitinib versus interferon alfa in metastatic renal-cell carcinoma. *N Engl J Med* 356: 115-124.
18. Al-Marrawi MY, Rini BI, Harshman LC, Bjarnason G, Wood L, et al. (2013) The association of clinical outcome to first-line VEGF-targeted therapy with clinical outcome to second-line VEGF-targeted therapy in metastatic renal cell carcinoma patients. *Target Oncol*.
19. Kessler ER, Bowles DW, Flaig TW, Lam ET, Jimeno A (2012) Axitinib, a new therapeutic option in renal cell carcinoma. *Drugs Today (Barc)* 48: 633-644.
20. Hara W, Tran P, Li G, Su Z, Puataweepong P, et al. (2009) Cyberknife for brain metastases of malignant melanoma and renal cell carcinoma. *Neurosurgery* 64: A26-32.
21. Abedalthagafi M, Bakhshwin A (2012) Radiation-induced glioma following CyberKnife(R) treatment of metastatic renal cell carcinoma: a case report. *J Med Case Rep* 6: 271.

22. O'Donoghue J (2004) Relevance of external beam dose-response relationships to kidney toxicity associated with radionuclide therapy. *Cancer Biother Radiopharm* 19: 378-387.
23. Goodhead DT (1989) The initial physical damage produced by ionizing radiations. *Int J Radiat Biol* 56: 623-634.
24. Merritt AJ, Allen TD, Potten CS, Hickman JA (1997) Apoptosis in small intestinal epithelial from p53-null mice: evidence for a delayed, p53-independent G2/M-associated cell death after gamma-irradiation. *Oncogene* 14: 2759-2766.
25. Suci D (1983) Cellular death by apoptosis in some radiosensitive and radioresistant mammalian tissues. *J Theor Biol* 105: 391-401.
26. Denison SH, May GS (1994) Mitotic catastrophe is the mechanism of lethality for mutations that confer mutagen sensitivity in *Aspergillus nidulans*. *Mutat Res* 304: 193-202.
27. Kabakov AE, Kudriavtsev VA, Makarova Iu M (2010) [Inhibitors of the heat shock protein 90 activity: a novel class of tumor radiosensitizers]. *Radiats Biol Radioecol* 50: 528-535.
28. Kastan MB, Onyekwere O, Sidransky D, Vogelstein B, Craig RW (1991) Participation of p53 protein in the cellular response to DNA damage. *Cancer Res* 51: 6304-6311.
29. Lehman AR, Stevens S (1977) The production and repair of double strand breaks in cells from normal humans and from patients with ataxia telangiectasia. *Biochim Biophys Acta* 474: 49-60.
30. Canman CE, Wolff AC, Chen CY, Fornace AJ, Jr., Kastan MB (1994) The p53-dependent G1 cell cycle checkpoint pathway and ataxia-telangiectasia. *Cancer Res* 54: 5054-5058.
31. DiGiovanna JJ, Kraemer KH (2012) Shining a light on xeroderma pigmentosum. *J Invest Dermatol* 132: 785-796.
32. Sasaki MS, Matsubara S (1977) Free radical scavenging in protection of human lymphocytes against chromosome aberration formation by gamma-ray irradiation. *Int J Radiat Biol Relat Stud Phys Chem Med* 32: 439-445.
33. Shiina T, Watanabe R, Shiraishi I, Suzuki M, Sugaya Y, et al. (2012) Induction of DNA damage, including abasic sites, in plasmid DNA by carbon ion and X-ray irradiation. *Radiat Environ Biophys*.
34. Herak JN, Galogaza V (1969) Radical transformation in irradiated DNA and its constituents. *Proc Natl Acad Sci U S A* 64: 8-12.
35. Barendsen GW (1964) Modification of Radiation Damage by Fractionation of the Dose, Anoxia, and Chemical Protectors in Relation to Let. *Ann N Y Acad Sci* 114: 96-114.
36. Schack JA, Macduffee RC (1949) Increased Radioresistance of Red Bone Marrow after Anoxia. *Science* 110: 259-260.
37. Gimbrone MA, Jr., Leapman SB, Cotran RS, Folkman J (1972) Tumor dormancy in vivo by prevention of neovascularization. *J Exp Med* 136: 261-276.
38. Blumenson LE, Bross ID (1976) A possible mechanism for enhancement of increased production of tumor angiogenic factor. *Growth* 40: 205-209.
39. Tannock IF (1968) The relation between cell proliferation and the vascular system in a transplanted mouse mammary tumour. *Br J Cancer* 22: 258-273.
40. Nyhan MJ, El Mashad SM, O'Donovan TR, Ahmad S, Collins C, et al. (2011) VHL genetic alteration in CCRCC does not determine de-regulation of HIF, CAIX, hnRNP A2/B1 and osteopontin. *Cell Oncol (Dordr)* 34: 225-234.
41. Leibovich BC, Sheinin Y, Lohse CM, Thompson RH, Cheville JC, et al. (2007) Carbonic anhydrase IX is not an independent predictor of outcome for patients with clear cell renal cell carcinoma. *J Clin Oncol* 25: 4757-4764.

42. Robertson N, Potter C, Harris AL (2004) Role of carbonic anhydrase IX in human tumor cell growth, survival, and invasion. *Cancer Res* 64: 6160-6165.
43. Brockton NT, Klimowicz AC, Bose P, Petrillo SK, Konno M, et al. (2012) High stromal carbonic anhydrase IX expression is associated with nodal metastasis and decreased survival in patients with surgically-treated oral cavity squamous cell carcinoma. *Oral Oncol* 48: 615-622.
44. Badger MR, Price GD (1994) The Role of Carbonic Anhydrase in Photosynthesis. *Ann Rev Plant Phys* 45: 369-392.
45. Lindskog S (1997) Structure and mechanism of carbonic anhydrase. *Pharmacol Ther* 74: 1-20.
46. Hewett-Emmett D, Tashian RE (1996) Functional diversity, conservation, and convergence in the evolution of the alpha-, beta-, and gamma-carbonic anhydrase gene families. *Mol Phylogenet Evol* 5: 50-77.
47. Syrjanen L, Tolvanen M, Hilvo M, Olatubosun A, Innocenti A, et al. (2010) Characterization of the first beta-class carbonic anhydrase from an arthropod (*Drosophila melanogaster*) and phylogenetic analysis of beta-class carbonic anhydrases in invertebrates. *BMC Biochem* 11: 28.
48. Ferry JG (2010) The gamma class of carbonic anhydrases. *Biochim Biophys Acta* 1804: 374-381.
49. Cox EH, McLendon GL, Morel FM, Lane TW, Prince RC, et al. (2000) The active site structure of *Thalassiosira weissflogii* carbonic anhydrase 1. *Biochemistry* 39: 12128-12130.
50. Breton S (2001) The cellular physiology of carbonic anhydrases. *JOP* 2: 159-164.
51. Supuran CT (2008) Carbonic anhydrases: novel therapeutic applications for inhibitors and activators. *Nat Rev Drug Discov* 7: 168-181.
52. Lovejoy DA, Hewett-Emmett D, Porter CA, Cepoi D, Sheffield A, et al. (1998) Evolutionarily conserved, "acatalytic" carbonic anhydrase-related protein XI contains a sequence motif present in the neuropeptide sauvagine: the human CA-RP XI gene (CA11) is embedded between the secretor gene cluster and the DBP gene at 19q13.3. *Genomics* 54: 484-493.
53. Hilvo M, Baranauskiene L, Salzano AM, Scaloni A, Matulis D, et al. (2008) Biochemical characterization of CA IX, one of the most active carbonic anhydrase isozymes. *J Biol Chem* 283: 27799-27809.
54. Alterio V, Hilvo M, Di Fiore A, Supuran CT, Pan P, et al. (2009) Crystal structure of the catalytic domain of the tumor-associated human carbonic anhydrase IX. *Proc Natl Acad Sci U S A* 106: 16233-16238.
55. Innocenti A, Pastorekova S, Pastorek J, Scozzafava A, De Simone G, et al. (2009) The proteoglycan region of the tumor-associated carbonic anhydrase isoform IX acts as an intrinsic buffer optimizing CO₂ hydration at acidic pH values characteristic of solid tumors. *Bioorg Med Chem Lett* 19: 5825-5828.
56. Ditte P, Dequiedt F, Svastova E, Hulikova A, Ohradanova-Repic A, et al. (2011) Phosphorylation of carbonic anhydrase IX controls its ability to mediate extracellular acidification in hypoxic tumors. *Cancer Res* 71: 7558-7567.
57. Supuran CT (2008) Carbonic anhydrases--an overview. *Curr Pharm Des* 14: 603-614.
58. Barathova M, Takacova M, Holotnakova T, Gibadulinova A, Ohradanova A, et al. (2008) Alternative splicing variant of the hypoxia marker carbonic anhydrase IX expressed independently of hypoxia and tumour phenotype. *Br J Cancer* 98: 129-136.

59. Opavsky R, Pastorekova S, Zelnik V, Gibadulinova A, Stanbridge EJ, et al. (1996) Human MN/CA9 gene, a novel member of the carbonic anhydrase family: structure and exon to protein domain relationships. *Genomics* 33: 480-487.
60. Wykoff CC, Beasley NJ, Watson PH, Turner KJ, Pastorek J, et al. (2000) Hypoxia-inducible expression of tumor-associated carbonic anhydrases. *Cancer Res* 60: 7075-7083.
61. Gimenez-Bachs JM, Salinas-Sanchez AS, Sanchez-Sanchez F, Lorenzo-Romero JG, Donate-Moreno MJ, et al. (2006) Determination of vhl gene mutations in sporadic renal cell carcinoma. *Eur Urol* 49: 1051-1057.
62. Chrastina A (2003) High cell density-mediated pericellular hypoxia is a crucial factor inducing expression of the intrinsic hypoxia marker CA IX in vitro in HeLa cells. *Neoplasma* 50: 251-256.
63. Semenza GL (2007) Hypoxia and cancer. *Cancer Metastasis Rev* 26: 223-224.
64. Thiry A, Dogne JM, Masereel B, Supuran CT (2006) Targeting tumor-associated carbonic anhydrase IX in cancer therapy. *Trends Pharmacol Sci* 27: 566-573.
65. Jaakkola P, Mole DR, Tian YM, Wilson MI, Gielbert J, et al. (2001) Targeting of HIF-alpha to the von Hippel-Lindau ubiquitylation complex by O₂-regulated prolyl hydroxylation. *Science* 292: 468-472.
66. Maxwell PH, Wiesener MS, Chang GW, Clifford SC, Vaux EC, et al. (1999) The tumour suppressor protein VHL targets hypoxia-inducible factors for oxygen-dependent proteolysis. *Nature* 399: 271-275.
67. Ratcliffe PJ, Pugh CW, Maxwell PH (2000) Targeting tumors through the HIF system. *Nat Med* 6: 1315-1316.
68. Potter C, Harris AL (2004) Hypoxia inducible carbonic anhydrase IX, marker of tumour hypoxia, survival pathway and therapy target. *Cell Cycle* 3: 164-167.
69. Ebbesen P, Pettersen EO, Gorr TA, Jobst G, Williams K, et al. (2009) Taking advantage of tumor cell adaptations to hypoxia for developing new tumor markers and treatment strategies. *J Enzyme Inhib Med Chem* 24 Suppl 1: 1-39.
70. Svastova E, Hulikova A, Rafajova M, Zat'ovicova M, Gibadulinova A, et al. (2004) Hypoxia activates the capacity of tumor-associated carbonic anhydrase IX to acidify extracellular pH. *FEBS Lett* 577: 439-445.
71. Supuran CT, Vullo D, Manole G, Casini A, Scozzafava A (2004) Designing of novel carbonic anhydrase inhibitors and activators. *Curr Med Chem Cardiovasc Hematol Agents* 2: 49-68.
72. Svastova E, Zilka N, Zat'ovicova M, Gibadulinova A, Ciampor F, et al. (2003) Carbonic anhydrase IX reduces E-cadherin-mediated adhesion of MDCK cells via interaction with beta-catenin. *Exp Cell Res* 290: 332-345.
73. Radvak P, Repic M, Svastova E, Takacova M, Csaderova L, et al. (2013) Suppression of carbonic anhydrase IX leads to aberrant focal adhesion and decreased invasion of tumor cells. *Oncol Rep*.
74. Dorai T, Sawczuk IS, Pastorek J, Wiernik PH, Dutcher JP (2005) The role of carbonic anhydrase IX overexpression in kidney cancer. *Eur J Cancer* 41: 2935-2947.
75. Akurathi V, Dubois L, Lieuwes NG, Chitneni SK, Cleynhens BJ, et al. (2010) Synthesis and biological evaluation of a ^{99m}Tc-labelled sulfonamide conjugate for in vivo visualization of carbonic anhydrase IX expression in tumor hypoxia. *Nucl Med Biol* 37: 557-564.

76. Neuman MG, Shear NH, Malkiewicz IM, Taeri M, Shapiro LE, et al. (2007) Immunopathogenesis of hypersensitivity syndrome reactions to sulfonamides. *Transl Res* 149: 243-253.
77. Cianchi F, Vinci MC, Supuran CT, Peruzzi B, De Giuli P, et al. (2010) Selective inhibition of carbonic anhydrase IX decreases cell proliferation and induces ceramide-mediated apoptosis in human cancer cells. *J Pharmacol Exp Ther* 334: 710-719.
78. Bernstein E, Caudy AA, Hammond SM, Hannon GJ (2001) Role for a bidentate ribonuclease in the initiation step of RNA interference. *Nature* 409: 363-366.
79. Hutvagner G, Zamore PD (2002) A microRNA in a multiple-turnover RNAi enzyme complex. *Science* 297: 2056-2060.
80. Lai EC, Wiel C, Rubin GM (2004) Complementary miRNA pairs suggest a regulatory role for miRNA:miRNA duplexes. *RNA* 10: 171-175.
81. Lindbo JA, Dougherty WG (1992) Untranslatable transcripts of the tobacco etch virus coat protein gene sequence can interfere with tobacco etch virus replication in transgenic plants and protoplasts. *Virology* 189: 725-733.
82. Kawasaki H, Taira K (2003) Short hairpin type of dsRNAs that are controlled by tRNA(Val) promoter significantly induce RNAi-mediated gene silencing in the cytoplasm of human cells. *Nucleic Acids Res* 31: 700-707.
83. Friedenstein AJ, Gorskaja JF, Kulagina NN (1976) Fibroblast precursors in normal and irradiated mouse hematopoietic organs. *Exp Hematol* 4: 267-274.
84. Powers EL (1962) Considerations of survival curves and target theory. *Phys Med Biol* 7: 3-28.
85. Iliopoulos O, Kibel A, Gray S, Kaelin WG, Jr. (1995) Tumour suppression by the human von Hippel-Lindau gene product. *Nat Med* 1: 822-826.
86. Kim M, Yan Y, Lee K, Sgagias M, Cowan KH (2004) Ectopic expression of von Hippel-Lindau tumor suppressor induces apoptosis in 786-O renal cell carcinoma cells and regresses tumor growth of 786-O cells in nude mouse. *Biochem Biophys Res Commun* 320: 945-950.
87. Shinojima T, Oya M, Takayanagi A, Mizuno R, Shimizu N, et al. (2007) Renal cancer cells lacking hypoxia inducible factor (HIF)-1 α expression maintain vascular endothelial growth factor expression through HIF-2 α . *Carcinogenesis* 28: 529-536.
88. Naves R, Lennon AM, Barbieri G, Reyes L, Puga G, et al. (2002) MHC class II-deficient tumor cell lines with a defective expression of the class II transactivator. *Int Immunol* 14: 481-491.
89. Hashmi S, Allderdice PW, Klein G, Miller OJ (1974) Chromosomal heterogeneity in the RAG and MSWBS mouse tumor cell lines. *Cancer Res* 34: 79-88.
90. Ou YC, Gardner TA, Kao C, Zhou HE, Chung LW (2005) A potential for tissue restrictive gene therapy in renal cell carcinoma using MN/CA IX promoter. *Anticancer Res* 25: 881-886.
91. Leith JT (1994) In vitro radiation sensitivity of the LNCaP prostatic tumor cell line. *Prostate* 24: 119-124.
92. Garzotto M, Haimovitz-Friedman A, Liao WC, White-Jones M, Huryk R, et al. (1999) Reversal of radiation resistance in LNCaP cells by targeting apoptosis through ceramide synthase. *Cancer Res* 59: 5194-5201.
93. Sheta EA, Trout H, Gildea JJ, Harding MA, Theodorescu D (2001) Cell density mediated pericellular hypoxia leads to induction of HIF-1 α via nitric oxide and Ras/MAP kinase mediated signaling pathways. *Oncogene* 20: 7624-7634.

94. Barazzuol L, Jena R, Burnet NG, Jeynes JC, Merchant MJ, et al. (2012) In vitro evaluation of combined temozolomide and radiotherapy using X rays and high-linear energy transfer radiation for glioblastoma. *Radiat Res* 177: 651-662.
95. Sudheerkumar P, Shiras A, Das G, Jagtap JC, Prasad V, et al. (2008) Independent activation of Akt and NF-kappaB pathways and their role in resistance to TNF-alpha mediated cytotoxicity in gliomas. *Mol Carcinog* 47: 126-136.
96. Proescholdt MA, Merrill MJ, Stoerr EM, Lohmeier A, Pohl F, et al. (2012) Function of carbonic anhydrase IX in glioblastoma multiforme. *Neuro Oncol* 14: 1357-1366.
97. Carbone L (2012) The utility of basic animal research. *Hastings Cent Rep Suppl*: S12-15.
98. Borden EC (1974) Viruses and breast cancer: implications of mouse and human studies. *Johns Hopkins Med J* 134: 66-76.
99. Huynh AS, Abrahams DF, Torres MS, Baldwin MK, Gillies RJ, et al. (2011) Development of an orthotopic human pancreatic cancer xenograft model using ultrasound guided injection of cells. *PLoS One* 6: e20330.
100. Rutkowski MR, Stephen TL, Conejo-Garcia JR (2012) Anti-tumor immunity: myeloid leukocytes control the immune landscape. *Cell Immunol* 278: 21-26.
101. Deutschmann SM, Kavermann H, Knack Y (2010) Validation of a NAT-based Mycoplasma assay according European Pharmacopoeia. *Biologicals* 38: 238-248.
102. Chou TC, Talalay P (1984) Quantitative analysis of dose-effect relationships: the combined effects of multiple drugs or enzyme inhibitors. *Adv Enzyme Regul* 22: 27-55.
103. Uemura H, Nakagawa Y, Yoshida K, Saga S, Yoshikawa K, et al. (1999) MN/CA IX/G250 as a potential target for immunotherapy of renal cell carcinomas. *Br J Cancer* 81: 741-746.
104. Hu Q, Hill RP (1996) Radiosensitivity, apoptosis and repair of DNA double-strand breaks in radiation-sensitive Chinese hamster ovary cell mutants treated at different dose rates. *Radiat Res* 146: 636-645.
105. Kivela A, Parkkila S, Saarnio J, Karttunen TJ, Kivela J, et al. (2000) Expression of a novel transmembrane carbonic anhydrase isozyme XII in normal human gut and colorectal tumors. *Am J Pathol* 156: 577-584.

Appendices

Appendix A: SDS-PAGE and Western blot components

Table 1. SDS-PAGE gel components and concentrations

	Separating Gel (8%)	Stacking Gel
Acrylamide/Bisacrylamide	1.13 M	1.41 M
Tris pH 8.8	0.375 M	
Tris pH 6.8		0.125 M
SDS	0.0347 M	0.0347 M
APS	3.29×10^{-6} M	6.57×10^{-6} M
TEMED	0.0100 M	0.0167 M

Table 2. SDS-PAGE buffers components and concentrations

	Running Buffer	Transfer Buffer
Tris	0.025 M	0.0480 M
Glycine	0.192 M	0.0390 M
SDS	0.00173 M	0.00129 M
Methanol		4.94 M

Table 3. Antibodies used

Target	Type	Provider	Cat. #	Dilution
Carbonic Anhydrase 9	Primary (Rabbit)	Epitomics	3829-1	1:1000
Pan Actin	Primary (Mouse)	NeoMarkers	MS-1295-P	1:1000
Anti-Rabbit	Secondary	Jackson ImmunoResearch	111-035-003	1:1000
Anti-Mouse	Secondary	Santa Cruz Biotechnology	SC-2031	1:1000

Appendix B: *Mycoplasma* DAPI assay

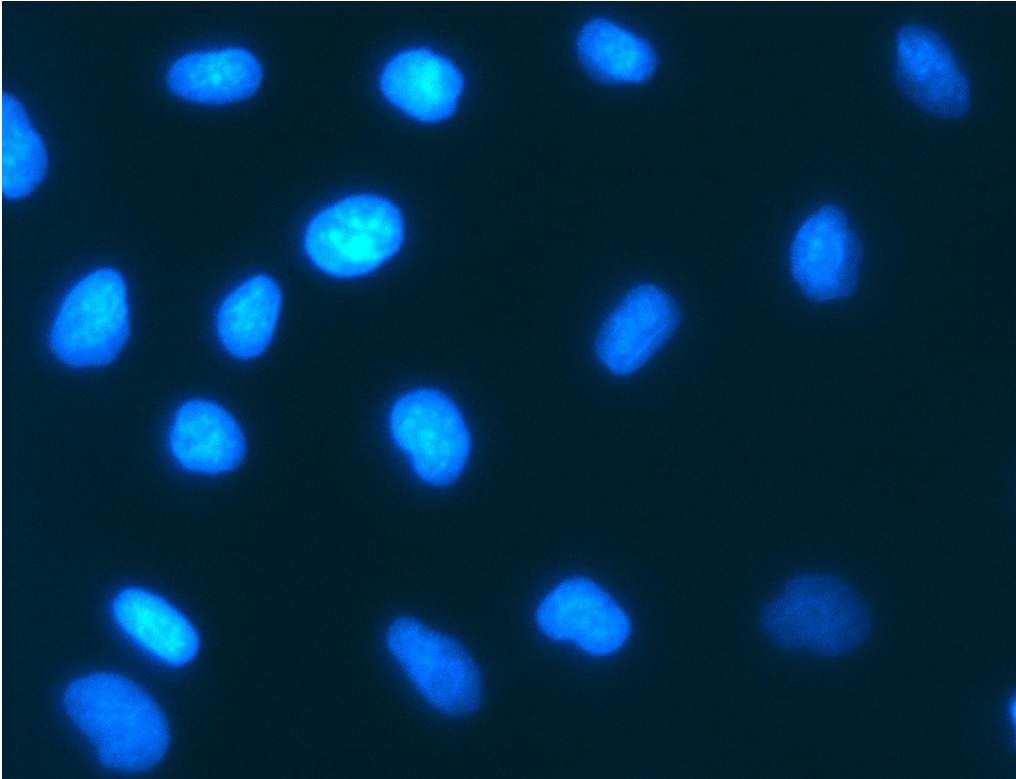


Fig. 17a. Fluorescence microscopy image of DAPI-stained 786-O cells (400x magnification). The cells were uninfected with *Mycoplasma* as indicated by the clear background. The nuclei stain blue.

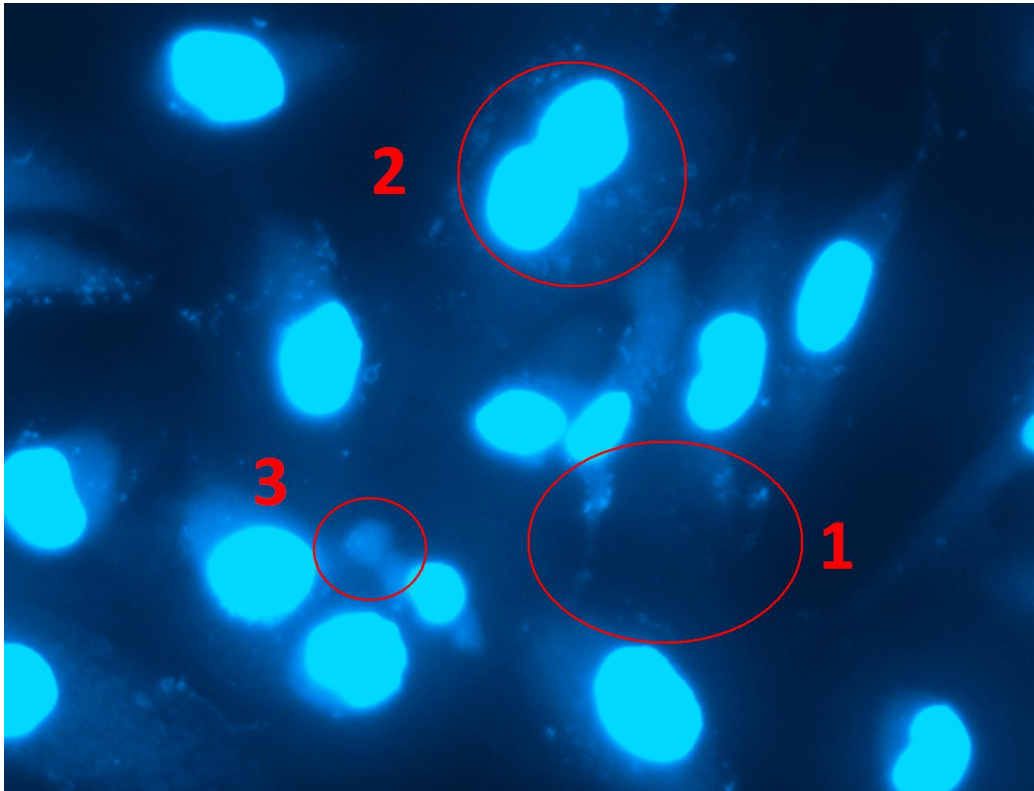


Fig. 17b. Fluorescence microscopy image of DAPI stained 786-O cells (brightness enhanced, 400x magnification). Signs of *Mycoplasma* infection in cell culture include 1) small speckled areas of staining, mostly inside but also beyond the cells' adherent areas 2) an abnormally high amount of large, multinucleated cells and 3) positively-stained cytoplasm, often with well-defined borders.

Appendix C: ShRNA Sequences

Table 4. Transfected shRNA sequences and targets

Vector	Sequence of shRNA Produced	Target in mRNA
GI356993	GGATGACCAGAGTCATTGGCGCTATGGAG	CA9 exon 2, catalytic domain, nucleotides 447–475
GI356994	ATGAGCAGTTGCTGTCTCGCTTGGAAGAA	CA9 exon 6, catalytic domain, nucleotides 908–936
GI356995	GTCACTGCTGCTTCTGATGCCTGTCCATC	CA9 exon 1, proteoglycan-like domain, nucleotides 123–151
GI356996*	GAACTTCCGAGCGACGCAGCCTTTGAATG	CA9 exon 8, catalytic domain, nucleotides 1161–1189
TR30013	GCACTACCAGAGCTAACTCAGATAGTACT	not effective found by BLAST (scrambled control)

* Plasmid used to create final knockdown (shCA9) subclone